Inorganic Chemistry

Article

Forum

Azide Groups in Higher Oxidation State Manganese Cluster Chemistry: From Structural Aesthetics to Single-Molecule Magnets

Theocharis C. Stamatatos and George Christou*

Department of Chemistry, University of Florida, Gainesville, Florida 32611-7200

This Forum Article overviews the recent amalgamation of two long-established areas, manganese/oxo coordination cluster chemistry involving the higher Mn^{II}/Mn^{IV} oxidation states and transition-metal azide (N_3^-) chemistry. The combination of azide and alkoxide- or carboxylate-containing ligands in Mn chemistry has led to a variety of new polynuclear clusters, high-spin molecules, and single-molecule magnets, with metal nuclearities ranging from Mn_4 to Mn_{32} and with ground-state spin values as large as $S = {}^{83}/_2$. The organic bridging/chelating ligands are discussed separately as follows: (i) pyridyl alkoxides [the anions of 2-(hydroxymethyl)pyridine (hmpH), 2,6-pyridinedimethanol (pdmH₂), and the *gem*-diol form of di-2-pyridyl ketone (dpkdH₂)]; (ii) non-pyridyl alkoxides [the anions of 1,1,1-tris(hydroxymethyl)ethane (thmeH₃), triethanolamine (teaH₃), and *N*-methyldiethanolamine (mdaH₂)]; (iii) other alcohols [the anions of 2,6-dihydroxymethyl-4-methylphenol (LH₃) and Schiff bases]; (iv) pyridyl monoximes/dioximes [the anions of methyl-2-pyridyl ketone oxime (mpkoH), phenyl-2-pyridyl ketone oxime (ppkoH), and 2,6-diacetylpyridine dioxime (dapdoH₂)]; (v) non-pyridyl oximes [the anions of salicylaldoxime (saoH₂) and its derivatives R-saoH₂]. The large structural diversity of the resulting complexes stems from the combined ability of the azide and organic ligands to adopt a variety of ligation and bridging modes. The combined work demonstrates the synthetic novelty that arises when azide is used in conjunction with alcohol-based chelates, the aesthetic beauty of the resulting molecules, and the often fascinating magnetic properties that these compounds possess. This continues to emphasize the extensive and remarkable ability of Mn chemistry to satisfy a variety of different tastes.

Introduction

The fascination of inorganic chemists with Mn coordination chemistry over the last 2 decades or so has been primarily driven by their relevance to two fields: The first is biomimetic, seeking the preparation of synthetic models for the structure, spectroscopic properties, and/or function of the active sites of several Mn redox enzymes, the most fascinating of which is the water-oxidizing complex of green plants and cyanobacteria, which is a Mn_4Ca species.[1] The second, with which this Forum Article is concerned, stems from the recognition that polynuclear Mn clusters containing Mn^{III} atoms will often possess large and even abnormally large ground-state spin (S) values, which combined with a large and negative magnetoanisotropy (as reflected in a large and negative zero-field-splitting parameter, D) have led to some

of these species functioning as single-molecule magnets (SMMs).[2] SMMs have a significant energy barrier (vs kT, where k is the Boltzmann constant) to magnetization relaxation, and the upper limit to the barrier (U) is given by $S^2|D|$ or $(S^2 - {}^1/_4)|D|$ for integer and half-integer spin, respectively.

SMMs represent a molecular or "bottom-up" approach to nanoscale magnetic materials.[3] Such molecules display the superparamagnetic properties normally associated with much larger magnetic particles, and they can therefore function as magnets below their blocking temperature, T_B, exhibiting magnetization hysteresis in applied direct current (dc) field sweeps.[4] Being molecular, SMMs differ fundamentally from traditional or "top-down" nanoscale magnets composed of metals, metal alloys, metal oxides (i.e., Fe, Fe_3O_4, CrO_2), etc. Indeed, they bring to nanomagnetism all of the advantages of molecular chemistry, including monodispersity,

* To whom correspondence should be addressed. E-mail: christou@chem.ufl.edu.

(1) (a) Ferreira, K. N.; Iverson, T. M.; Maghlaoui, K.; Barber, J.; Iwata, S. *Science* **2004**, *303*, 1831. (b) Carrell, T. G.; Tyryshkin, A. M.; Dismukes, G. C. *J. Biol. Inorg. Chem.* **2002**, *7*, 2. (c) Cinco, R. M.; Rompel, A.; Visser, H.; Aromi, G.; Christou, G.; Sauer, K.; Klein, M. P.; Yachandra, V. K. *Inorg. Chem.* **1999**, *38*, 5988. (d) Yachandra, V. K.; Sauer, K.; Klein, M. P. *Chem. Rev.* **1996**, *96*, 2927. (e) Yocum, C. F.; Pecoraro, V. L. *Curr. Opin. Chem. Biol.* **1999**, *3*, 182.

(2) For some representative references, see: (a) Christou, G.; Gatteschi, D.; Hendrickson, D. N.; Sessoli, R. *MRS Bull.* **2000**, *25*, 66. (b) Sessoli, R.; Tsai, H.-L.; Schake, A. R.; Wang, S.; Vincent, J. B.; Folting, K.; Gatteschi, D.; Christou, G.; Hendrickson, D. N. *J. Am. Chem. Soc.* **1993**, *115*, 1804.

(3) For a recent review, see: Christou, G. *Polyhedron* **2005**, *24*, 2065.

crystallinity, true solubility (rather than colloid formation), peripheral protection by a shell of organic groups that prevents close contact of a molecule's magnetic core with those of neighboring ones, and the ability to vary this organic shell at will using standard chemical methods.

SMMs have been proposed for several potential applications, such as (i) in very high-density information storage[5] and spintronics,[6] taking advantage of the magnetization orientation of a single molecule; (ii) in quantum computing, where each molecule would function as a quantum bit existing as a quantum superposition of states owing to the fact that it exhibits quantum tunneling of magnetization (QTM) through the anisotropy barrier to magnetization relaxation;[5] and (iii) magnetic resonance imaging contrast agents.[7] The demonstration of the classical macroscale property of magnetization hysteresis and the quantum properties of QTM and also quantum phase interference (Berry phase)[8] emphasizes that such molecules are mesoscale particles, truly straddling the classical/quantum interface.

To date, the most studied SMMs are the $[Mn_{12}O_{12}(O_2CR)_{16}(H_2O)_4]$ ($Mn^{III}_8Mn^{IV}_4$; R = various) family with an $S = 10$ ground state.[2,9] There are now also many other structural types displaying SMM behavior, the vast majority being Mn complexes owing to their often large S values and relatively large (and negative) D values arising from Jahn−Teller (JT)-distorted Mn^{III} atoms. However, the presence of Mn^{II} atoms, which give weak exchange interactions with Mn^{III}, often leads to SMMs with low-lying excited states and increased relaxation rates.[10] Thus, the SMMs with the largest relaxation barriers are currently either Mn^{III}_x or mixed-valent Mn^{III}/Mn^{IV} species. The former currently comprise Mn_2,[11] Mn_3,[12] Mn_4,[13] Mn_6,[14] Mn_{26},[15] and Mn_{84}[16] complexes, including the Mn_6 complex with the highest barrier yet discovered.[14c]

Synthetic procedures to new high-spin molecules are thus of continuing importance in order to discover new SMMs

and also for a fundamental understanding of high-spin species. Large S values can result from ferromagnetic (or ferrimagnetic) spin alignments and/or from competing antiferromagnetic interactions (spin frustration) in certain M_x topologies that prevent (frustrate) perfectly antiparallel spin alignments.[17,18] The former allows predictions about new topologies and structures that will lead to high-spin products (although then developing the targeted synthesis of such species is extremely challenging), whereas the latter permits few predictions for high-nuclearity clusters with many inequivalent exchange interactions.[19,20] Thus, one of our approaches to new high-spin complexes is to employ bridging
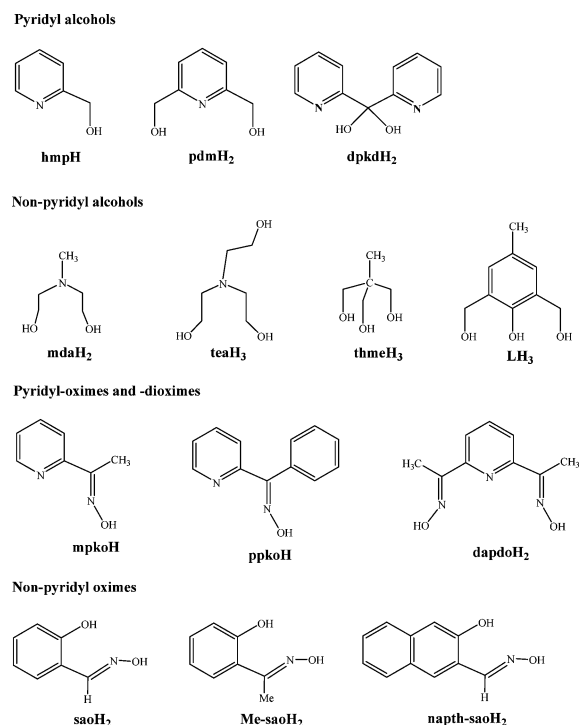
(4) (a) Bircher, R.; Chaboussant, G.; Dobe, D.; Güdel, H. U.; Oshsenbein, S. T.; Sieber, A.; Waldmann, O. *Adv. Funct. Mater.* **2006**, *16*, 209. (b) Gatteschi, D.; Sessoli, R. *Angew. Chem., Int. Ed.* **2003**, *42*, 268. (c) Aubin, S. M. J.; Gilley, N. R.; Pardi, L.; Krzystek, J.; Wemple, M. W.; Brunel, L.-C.; Maple, M. B.; Christou, G.; Hendrickson, D. N. *J. Am. Chem. Soc.* **1998**, *120*, 4991. (d) Oshio, H.; Nakano, M. *Chem.−Eur. J.* **2005**, *11*, 5178. (e) Sessoli, R.; Gatteschi, D.; Caneschi, A.; Novak, M. A. *Nature* **1993**, *365*, 141.

(5) (a) Friedman, J. R.; Sarachik, M. P.; Tejada, J.; Ziolo, R. *Phys. Rev. Lett.* **1996**, *76*, 3830. (b) Thomas, L.; Lionti, L.; Ballou, R.; Gatteschi, D.; Sessoli, R.; Barbara, B. *Nature* **1996**, *383*, 145. (c) Wernsdorfer, W.; Sessoli, R. *Science* **1999**, *284*, 133. (d) Soler, M.; Wernsdorfer, W.; Folting, K.; Pink, M.; Christou, G. *J. Am. Chem. Soc.* **2004**, *126*, 2156. (e) Canneschi, A.; Ohm, T.; Paulsen, C.; Rovai, D.; Sangregorio, C.; Sessoli, R. *J. Magn. Magn. Mater.* **1998**, *177*, 1330. (f) Barbara, B.; Wernsdorfer, W.; Sampaio, L. C.; Park, J. G.; Paulsen, C.; Novak, M. A.; Ferrer, R.; Mailly, D.; Sessoli, R.; Caneschi, A.; Hasselbach, K.; Benoit, A.; Thomas, L. *J. Magn. Magn. Mater.* **1995**, *140*, 1825.

(6) Bogani, L.; Wernsdorfer, W. *Nat. Mater.* **2008**, *7*, 179.

(7) (a) Rodriguez, E.; Roig, A.; Molins, E.; Arus, C.; Quintero, M. R.; Cabanas, M. E.; Cerdan, S.; Lopez-Larrubia, P.; Sanfeliu, C. *NMR Biomed.* **2005**, *18*, 300. (b) Isaacman, S.; Kumar, R.; del Barco, E.; Kent, A. D.; Canary, J. W.; Jerschow, A. *Polyhedron* **2005**, *24*, 2691. (c) Cage, B.; Russek, S. E.; Shoemaker, R.; Barker, A. J.; Stoldt, C.; Ramachandaran, V.; Dalal, N. S. *Polyhedron* **2007**, *26*, 2413.

(8) (a) Leuenberger, M. N.; Meier, F.; Loss, D. *Monatsh. Chem.* **2003**, *134*, 217. (b) Wernsdorfer, W.; Soler, M.; Christou, G.; Hendrickson, D. N. *J. Appl. Phys.* **2002**, *91*, 7164. (c) Wernsdorfer, W.; Chakov, N. E.; Christou, G. *Phys. Rev. Lett.* **2005**, *95*, 037203 (1−4). .

(9) (a) Lis, T. *Acta Crystallogr.* **1980**, *B36*, 2042. (b) Artus, P.; Boskovic, C.; Yoo, Y.; Streib, W. E.; Brunel, L.-C.; Hendrickson, D. N.; Christou, G. *Inorg. Chem.* **2001**, *40*, 4199. (c) Ruiz, D.; Sun, Z.; Albela, B.; Folting, K.; Ribas, J.; Christou, G.; Hendrickson, D. N. *Angew. Chem., Int. Ed.* **1998**, *37*, 300. (d) Aubin, S. M. J.; Sun, Z.; Guzei, I. A.; Rheingold, A. L.; Christou, G.; Hendrickson, D. N. *J. Chem. Soc., Chem. Commun.* **1997**, 2239. (e) Boskovic, C.; Pink, M.; Huffman, J. C.; Hendrickson, D. N.; Christou, G. *J. Am. Chem. Soc.* **2001**, *123*, 9914. (f) Soler, M.; Artus, P.; Folting, K.; Huffman, J. C.; Hendrickson, D. N.; Christou, G. *Inorg. Chem.* **2001**, *40*, 4902. (g) Chakov, N. E.; Abboud, K. A.; Zakharov, L. N.; Rheingold, A. L.; Hendrickson, D. N.; Christou, G. *Polyhedron* **2003**, *22*, 1759. (h) Chakov, N. E.; Lawrence, J.; Harter, A. G.; Hill, S. O.; Dalal, N. S.; Wernsdorfer, W.; Abboud, K. A.; Christou, G. *J. Am. Chem. Soc.* **2006**, *128*, 6975. (i) Bagai, R.; Christou, G. *Inorg. Chem.* **2007**, *46*, 10810.

(10) (a) Aliaga-Alcade, N.; Edwards, R. S.; Hill, S. O.; Wernsdorfer, W.; Folting, K.; Christou, G. *J. Am. Chem. Soc.* **2004**, *126*, 12503. (b) Yoo, J.; Brechin, E. K.; Yamaguchi, A.; Nakano, M.; Huffman, J. C.; Maniero, A. L.; Brunel, L.-C.; Awaga, K.; Ishimoto, H.; Christou, G.; Hendrickson, D. N. *Inorg. Chem.* **2000**, *39*, 3615. (c) Brechin, E. K.; Yoo, J.; Nakano, M.; Huffman, J. C.; Hendrickson, D. N.; Christou, G. *Chem. Commun.* **1999**, 783. (d) Wang, S.; Wemple, M. S.; Tsai, H.-L.; Folting, K.; Huffman, J. C.; Hagen, K. S.; Hendrickson, D. N.; Christou, G. *Inorg. Chem.* **2000**, *39*, 1501. (e) Wemple, M. W.; Tsai, H.-L.; Folting, K.; Hendrickson, D. N.; Christou, G. *Inorg. Chem.* **1993**, *32*, 2025. (f) Aliaga, N.; Folting, K.; Hendrickson, D. N.; Christou, G. *Polyhedron* **2001**, *20*, 1273.

(11) (a) Rajaraman, G.; Sanudo, E. C.; Helliwell, M.; Piligkos, S.; Wernsdorfer, W.; Christou, G.; Brechin, E. K. *Polyhedron* **2005**, *24*, 2450. (b) Miyasaka, H.; Clérac, R.; Wernsdorfer, W.; Lecren, L.; Bonhomme, C.; Sugiura, K.; Yamashita, M. *Angew. Chem., Int. Ed.* **2004**, *43*, 2801.

(12) (a) Stamatatos, Th. C.; Foguet-Albiol, D.; Stoumpos, C. C.; Raptopoulou, C. P.; Terzis, A; Wernsdorfer, W.; Perlepes, S. P.; Christou, G. *J. Am. Chem. Soc.* **2005**, *127*, 15380. (b) Stamatatos, Th. C.; Foguet-Albiol, D.; Lee, S.-C.; Stoumpos, C. C.; Raptopoulou, C. P.; Terzis, A.; Wernsdorfer, W.; Hill, S.; Perlepes, S. P.; Christou, G. *J. Am. Chem. Soc.* **2007**, *129*, 9484.

(13) Milios, C. J.; Prescimone, A.; Mishra, A.; Parsons, S.; Wernsdorfer, W.; Christou, G.; Perlepes, S. P.; Brechin, E. K. *Chem. Commun.* **2007**, 153.

(14) (a) Milios, C. J.; Raptopoulou, C. P.; Terzis, A.; Lloret, F.; Vicente, R.; Perlepes, S. P.; Escuer, A. *Angew. Chem., Int. Ed.* **2004**, *43*, 210. (b) Milios, C. J.; Vinslava, A.; Wood, P. A.; Parsons, S.; Wernsdorfer, W.; Christou, G.; Perlepes, S. P.; Brechin, E. K. *J. Am. Chem. Soc.* **2007**, *129*, 8. (c) Milios, C. J.; Vinslava, A.; Wernsdorfer, W.; Moggach, S.; Parsons, S.; Perlepes, S. P.; Christou, G.; Brechin, E. K. *J. Am. Chem. Soc.* **2007**, *129*, 2754.

(15) Jones, L. F.; Rajaraman, G.; Brockman, J.; Murugescu, M.; Sanudo, E. C.; Raftery, J.; Teat, S. J.; Wernsdorfer, W.; Christou, G.; Brechin, E. K.; Collison, D. *Chem.−Eur. J.* **2004**, *10*, 5180.

(16) Tasiopoulos, A. J.; Vinslava, A.; Wernsdorfer, W.; Abboud, K. A.; Christou, G. *Angew. Chem., Int. Ed.* **2004**, *43*, 2117.

(17) (a) Stamatatos, Th. C.; Christou, G. *Philos. Trans. R. Soc. A* **2008**, *366*, 113, and references cited therein. (b) Aromi, G.; Knapp, M. J.; Claude, J.-P.; Huffman, J. C.; Hendrickson, D. N.; Christou, G. *J. Am. Chem. Soc.* **1999**, *121*, 5489.

(18) Kahn, O. *Molecular Magnetism*; VCH Publishers: New York, 1993.

(19) (a) Stamatatos, Th. C.; Abboud, K. A.; Wernsdorfer, W.; Christou, G. *Angew. Chem., Int. Ed.* **2007**, *46*, 884. (b) Boudalis, A. K.; Donnadieu, B.; Nastopoulos, V.; Clemente-Juan, J.; Modesto, M.; Alain; Yiannis, T.; Jean-Pierre; Perlepes, S. P. *Angew. Chem., Int. Ed.* **2004**, *43*, 2266.

Scheme 1. Crystallographically Established Coordination Modes of the Azide Ligand in Transition-Metal Complexes

Scheme 2. Protonated Precursors to the Chelating Ligands Discussed in the Text
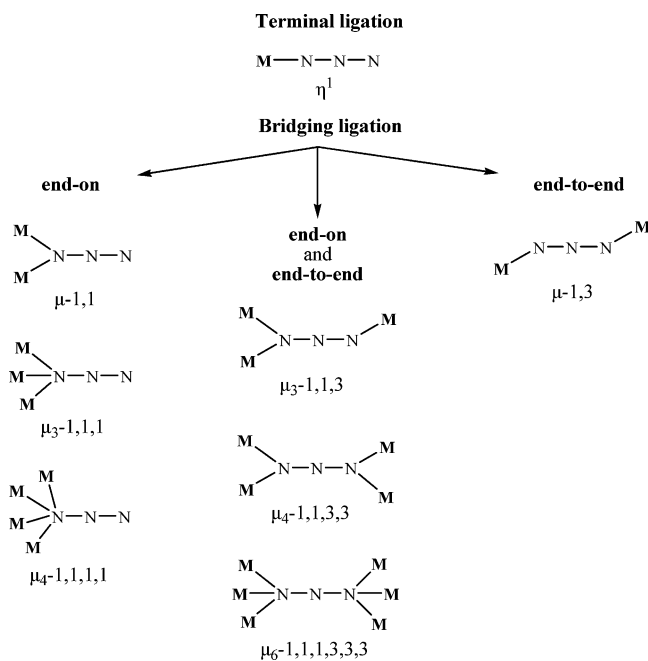
ligands that typically give ferromagnetic interactions and which can thus increase the chances of a large ground-state S value.

In the majority of polynuclear Mn complexes, exchange interactions are mainly propagated by bridging O^{2-}, OH^-, OR^-, or RCO_2^- groups (or a combination of these), ligands that usually lead to antiferromagnetic coupling.[18] However, the azide (N_3^-) group bridging in the 1,1-fashion (end-on) mode gives a ferromagnetic interaction for a wide range of M−N−M angles.[21] Azide ligands have been widely employed in dinuclear transition-metal compounds and as part of one-, two-, or three-dimensional extended networks,[22] where the N_3^- ion has been found to exhibit a wide variety of coordination modes (Scheme 1).[21a] It is thus an already well-recognized route to high-spin species and SMMs, although its use in Mn^{III}-containing cluster chemistry is still in its infancy.

Similarly, we and others have had a longstanding interest in the use of alkoxide-based chelating ligands in Mn cluster chemistry, including the anions of 2-(hydroxymethyl)pyridine (hmpH),[23] 2,6-pyridinedimethanol (pdmH$_2$),[24] and the *gem*-diolate form of di-2-pyridyl ketone, (py)$_2$C(O)$_2^{2-}$ (dpkd^{2-}),[25] formed in situ from dpk [dpk = (py)$_2$CO; dpkdH$_2$ = (py)$_2$C(OH)$_2$; Scheme 2]. These and related ones such as the anions of 1,1,1-tris(hydroxymethyl)ethane (thmeH$_3$),[26] tri-

ethanolamine (teaH$_3$),[27] N-methyldiethanolamine (mdaH$_2$)[28] and others (Scheme 2) are excellent bridging units that can yield high-nuclearity products. From a magnetic point of

(20) (a) Papaefstathiou, G. S.; Perlepes, S. P.; Escuer, A.; Vicente, R.; Font-Bardia, M.; Solans, X. *Angew. Chem., Int. Ed.* **2001**, *40*, 884. (b) Papaefstathiou, G. S.; Escuer, A.; Vicente, R.; Font-Bardia, M.; Solans, X.; Perlepes, S. P. *Chem. Commun.* **2001**, 2414.

(21) (a) Escuer, A.; Aromi, G. *Eur. J. Inorg. Chem.* **2006**, 4721, and references cited therein. (b) Ruiz, E.; Cano, J.; Alvarez, S.; Alemany, P. *J. Am.Chem. Soc.* **1998**, *120*, 11122.

(22) For a representative review, see: Ribas, J.; Escuer, A.; Monfort, M.; Vicente, R.; Cortes, R.; Lezama, L.; Rojo, T. *Coord. Chem. Rev.* **1999**, *193*, 195–1027, and references cited therein.

(23) For some representative references, see: (a) Harden, N. C.; Bolcar, M. A.; Wernsdorfer, W.; Abboud, K. A.; Streib, W. E.; Christou, G. *Inorg. Chem.* **2003**, *42*, 7067. (b) Yang, E.-C.; Harden, N.; Wernsdorfer, W.; Zakharov, L.; Brechin, E. K.; Rheingold, A. L.; Christou, G.; Hendrickson, D. N. *Polyhedron* **2003**, *22*, 1857. (c) Boskovic, C.; Brechin, E. K.; Streib, W. E.; Folting, K.; Bollinger, J. C.; Hendrickson, D. N.; Christou, G. *J. Am. Chem. Soc.* **2002**, *124*, 3725. (d) Lecren, L.; Roubeau, O.; Coulon, C.; Li, Y.-G.; Goff, X. F. L.; Wernsdorfer, W.; Miyasaka, H.; Clérac, R. *J. Am.Chem. Soc.* **2005**, *127*, 17353. (e) Lecren, L.; Wernsdorfer, W.; Li, Y.-G.; Roubeau, O.; Miyasaka, H.; Clérac, R. *J. Am. Chem. Soc.* **2005**, *127*, 11311. (f) Bolcar, M. A.; Aubin, S. M. J.; Folting, K.; Hendrickson, D. N.; Christou, G. *J. Chem. Soc., Chem. Commun.* **1997**, 1485.

(24) (a) Boskovic, C.; Wernsdorfer, W.; Folting, K.; Huffman, J. C.; Hendrickson, D. N.; Christou, G. *Inorg. Chem.* **2002**, *41*, 5107. (b) Murugesu, M.; Wernsdorfer, W.; Abboud, K. A.; Christou, G. *Polyhedron* **2005**, *24*, 2894. (c) Miyasaka, H.; Nakata, K.; Lecren, L.; Coulon, C.; Nakazawa, Y.; Fujisaki, T.; Sugiura, K.; Yamashita, M.; Clérac, R. *J. Am. Chem. Soc.* **2006**, *128*, 3770. (d) Murugesu, M.; Mishra, A.; Wernsdorfer, W.; Abboud, K. A.; Christou, G. *Polyhedron* **2006**, *25*, 613.

(25) (a) Milios, C. J.; Kefalloniti, E.; Raptopoulou, C. P.; Terzis, A.; Vicente, R.; Lalioti, N.; Escuer, A.; Perlepes, S. P. *Chem. Commun.* **2003**, 819. (b) Dendrinou-Samara, C.; Alexiou, M.; Zaleski, C. M.; Kampf, J. W.; Kirk, M. L.; Kessissoglou, D. P.; Pecoraro, V. L. *Angew. Chem., Int. Ed.* **2003**, *42*, 3763. (c) Zaleski, C. M.; Depperman, E. C.; Dendrinou-Samara, C.; Alexiou, M.; Kampf, J. W.; Kessissoglou, D. P.; Kirk, M. L.; Pecoraro, V. L. *J. Am. Chem. Soc.* **2005**, *127*, 12862.

(26) For a representative review, see: Brechin, E. K. *Chem. Commun.* **2005**, 5141, and references cited therein.

(27) (a) Murugesu, M.; Wernsdorfer, W.; Abboud, K. A.; Christou, G. *Angew. Chem., Int. Ed.* **2005**, *44*, 892, and references cited therein. (b) Pilawa, B.; Kelemen, M. T.; Wanka, S.; Geisselmann, A.; Barra, A. L. *Europhys. Lett.* **1998**, *43*, 7.

(28) (a) Foguet-Albiol, D.; O'Brien, T. A.; Wernsdorfer, W.; Moulton, B.; Zaworotko, M. J.; Abboud, K. A.; Christou, G. *Angew. Chem., Int. Ed.* **2005**, *44*, 897. (b) Saalfrank, R. W.; Nakajima, T.; Mooren, N.; Scheurer, A.; Maid, H.; Hampel, F.; Trieflinger, C.; Daub, J. *Eur. J. Inorg. Chem.* **2005**, 1149.
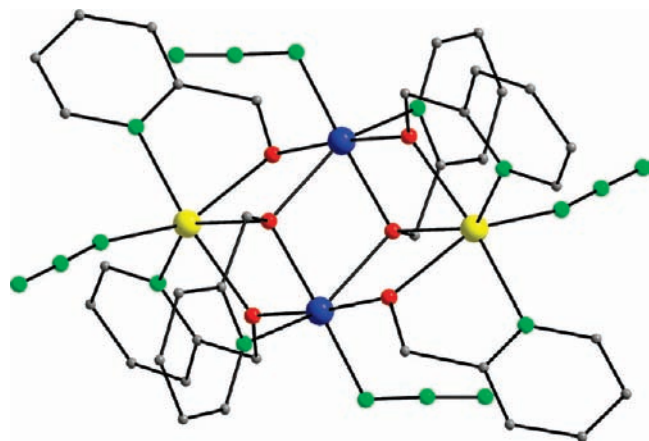
Figure 1. Molecular structure of complex **1**, with H atoms omitted for clarity. Color scheme: Mn^{II}, yellow; Mn^{III}, blue; O, red; N, green; C, gray.

view, their alkoxide arm(s) often support ferromagnetic coupling between the metal atoms that they bridge.

More recently, we have been investigating a number of other N- and O-based chelates. One family of these has been the 2-pyridyl oximes and particularly methyl-2-pyridyl ketone oxime (mpkoH)[12] and 2,6-diacetylpyridine dioxime (dapdoH$_2$);[29] these are shown in Scheme 2, where the analogy between the mpkoH/dapdoH$_2$ and hmpH/pdmH$_2$ pairs can clearly be seen. We recently reported, for example, the employment of mpkoH in manganese carboxylate chemistry, which gave the initial examples of triangular Mn^{III} SMMs by switching the exchange coupling from the more usual antiferromagnetic to ferromagnetic[12] and establishing the coordination affinity of 2-pyridyl oximato ligands toward Mn^{III}-containing products.

We shall herein overview our amalgamation in Mn^{III}-containing cluster chemistry of azides and the alkoxide or oximate chelates in Scheme 2. We shall thus be emphasizing our own efforts in this area but will also include results from other groups that have since employed the same or similar synthetic strategy in their work.

Results and Discussion

A. Mn Clusters of Azides and Alkoxide-Based Ligands. A.1. Pyridyl Alcohols. A.1.1. 2-(Hydroxymethyl)pyridine (hmpH). The early Mn cluster chemistry of hmpH and azide is dominated by tetranuclear, mixed-valence Mn^{II}/Mn^{III} complexes, such as [Mn$^{II}_2$Mn$^{III}_2$(N$_3$)$_4$(hmp)$_6$] (**1**) (Figure 1) and [Mn$^{II}_2$Mn$^{III}_2$Cl$_3$(N$_3$)(hmp)$_6$] (**2**), both with a planar Mn$_4$ rhombus topology and terminal azido groups.[30] A related compound is [Mn$^{II}_2$Mn$^{III}_2$(N$_3$)$_2$(hmp)$_6$]$_n^{2+}$ (**3**) (Figure 2), which is a one-dimensional chain with bridging μ-1,3-azido ligands.[23d] The magnetic properties of **1** and **2** reveal dominant ferromagnetic exchange interactions and a maximum possible ground state of $S = 9$ and establish that they are SMMs. Complex **3** is a chain of such species weakly antiferromagnetically coupled to each other through the azide

bridges with an exchange parameter of $J \approx -0.1$ K ($\mathscr{H} = -2J\hat{S}_i \cdot \hat{S}_j$ convention).

More recently, a slightly modified reaction led instead to two new decanuclear, mixed-valence clusters, [Mn$^{II}_4$Mn$^{III}_6$-O$_4$(N$_3$)$_4$(hmp)$_{12}$](X)$_2$ [X = ClO$_4^-$ (**4**), N$_3^-$ (**5**)] (Figure 3).[31] The [Mn$_{10}$(μ_4-O)$_4$(μ_3-N$_3$)$_4$]$^{14+}$ core of the cation has a tetraface-capped octahedral topology, with a central Mn$^{III}_6$ octahedron whose eight faces are bridged by four μ_3-N$_3^-$ and four μ_4-O^{2-} ions, the latter also bridging to four extrinsic Mn^{II} atoms and thus forming a Mn$^{II}_4$ tetrahedron above four nonadjacent faces of the octahedron. The μ_3-N$_3^-$ ions bind in the magnetically desirable μ_3-1,1,1 (end-on) fashion and yield ferromagnetic coupling between the Mn^{III} atoms of the central Mn$^{III}_6$ octahedron, whereas the 12 hmp$^-$ groups chelate each Mn^{II} atom and bridge with their alkoxide arms to different Mn^{III} atoms. As a result, the complete cation, which has rare T point group symmetry, is completely ferromagnetically coupled (Figure 4) with a resulting $S = 22$ ground state, one of the highest known. This was confirmed by fits of dc magnetization vs field (H) and temperature (T) data by matrix diagonalization, which gave $S = 22$, $g = 2.00$, and $D \approx 0.0$ cm^{-1}, thus establishing a high ground-state spin but with little or no anisotropy. The latter was expected from the high (cubic) symmetry of the molecule because, although Mn^{III} ions have significant single-ion anisotropy, the molecular anisotropy is the tensorial sum of the single-ion values, and this sum should be essentially zero given the cubic symmetry and the resulting orientations of the six Mn^{III} JT axes. The lack of anisotropy results in no out-of-phase ac magnetic susceptibility signal down to 1.8 K, indicating the absence of a significant barrier to magnetization relaxation; i.e., **4** and **5** are not SMMs.

A.1.2. 2,6-Pyridinedimethanol (pdmH$_2$). When pdmH$_2$ was employed in certain Mn/N$_3^-$ reactions, the main isolable product was tetranuclear [Mn$^{II}_2$Mn$^{III}_2$(N$_3$)$_4$(pdmH)$_6$] (**6**), again with a planar Mn$_4$ rhombus topology and terminal azido groups. Like complex **1**, complex **6** contains ferromagnetically coupled Mn atoms and an $S = 9$ ground state and exhibits out-of-phase alternating current (ac) susceptibility signals characteristic of an SMM (Figure 5).[30] The compound was obtained in high yields under a wide range of reaction conditions and reaction solvents such as MeCN, MeOH, and MeNO$_2$, among others. However, when a MeCN/MeOH mixture was employed, the product was instead a salt containing the new cation [Mn$_{25}$O$_{18}$(OH)$_2$(N$_3$)$_{12}$(pdm)$_6$-(pdmH)$_6$]$^{2+}$ (**7**).[32] The Mn$_{25}$ cation of **7** has a barrel-like cage structure involving 12 μ_4-O^{2-}, 6 μ_3-O^{2-}, and 2 μ_3-OH$^-$ ions and peripheral ligation consisting of chelating/bridging pdm^{2-}/pdmH$^-$ and both terminal and end-on bridging μ-1,1 N$_3^-$ groups; each of the latter bridges a Mn$^{II}\cdots$Mn^{III} pair. The core comprises five layers of three types with an **ABCBA** arrangement (Figure 6). Layer **A** is a Mn$^{II}_3$ triangular unit with a capping μ_3-OH$^-$ ion; layer **B** is a Mn$^{III}_6$

(29) Stamatatos, Th. C.; Luisi, B. S.; Moulton, B.; Christou, G. *Inorg. Chem.* **2008**, *47*, 1134.

(30) Stamatatos, Th. C.; Abboud, K. A.; Wernsdorfer, W.; Christou, G. Unpublished results.

(31) (a) Stamatatos, Th. C.; Abboud, K. A.; Wernsdorfer, W.; Christou, G. *Angew. Chem., Int. Ed.* **2006**, *45*, 4134. (b) Stamatatos, Th. C.; Abboud, K. A.; Wernsdorfer, W.; Christou, G. *Polyhedron* **2007**, *26*, 2042. (c) Stamatatos, Th. C.; Poole, K. M.; Abboud, K. A.; Wernsdorfer, W.; O'Brien, T. A.; Christou, G. *Inorg. Chem.* **2008**, *47*, 5006.
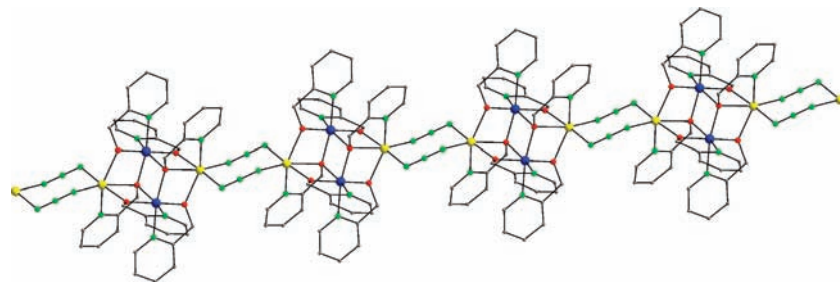
Figure 2. Molecular structure of the cation of complex **3**, with H atoms omitted for clarity. Color scheme: Mn^{II}, yellow; Mn^{III}, blue; O, red; N, green; C, gray.
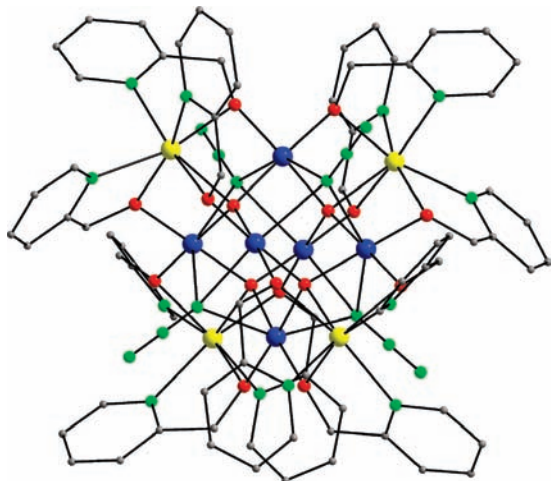

Figure 3. Molecular structure of the cation of complex **4**, with H atoms omitted for clarity. Color scheme: Mn^{II}, yellow; Mn^{III}, blue; O, red; N, green; C, gray.
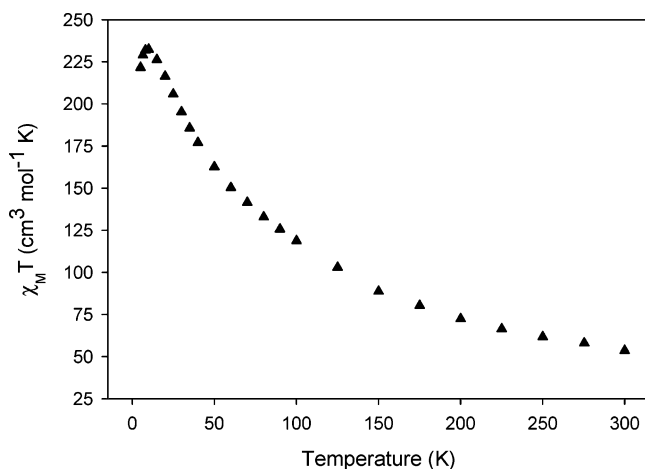

Figure 4. Plot of $\chi_M T$ vs T for complex **4** in a 1 kG dc field.

triangle comprising three corner-sharing Mn^{III}_3 triangles; and layer **C** is a Mn^{III}_6 hexagon with a central Mn^{IV} ion. Each layer is held together and linked to its neighboring layers by a combination of O^{2-}, OR^-, and/or N_3^- bridges.

The mixed-valent cluster **7** is one of the biggest yet synthesized in Mn chemistry, and it has a large spin of $S = {}^{51}/_2$ but a small anisotropy of $D = -0.020$ cm^{-1}, as determined by high-frequency electron paramagnetic resonance and fits of magnetization versus field and temperature data, with the latter using small applied fields to avoid

(32) Murugesu, M.; Habrych, M.; Wernsdorfer, W.; Abboud, K. A.; Christou, G. *J. Am. Chem. Soc.* **2004**, *126*, 4766.
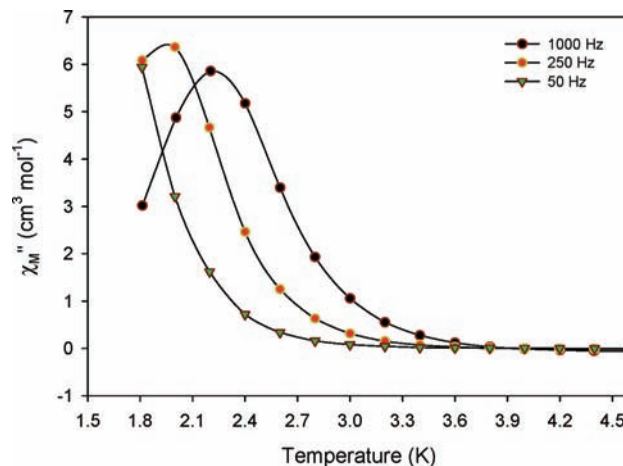
Figure 5. Plot of the out-of-phase (χ''_M) ac susceptibility signals of complex **6** in a 3.5 G field oscillating at the indicated frequencies.
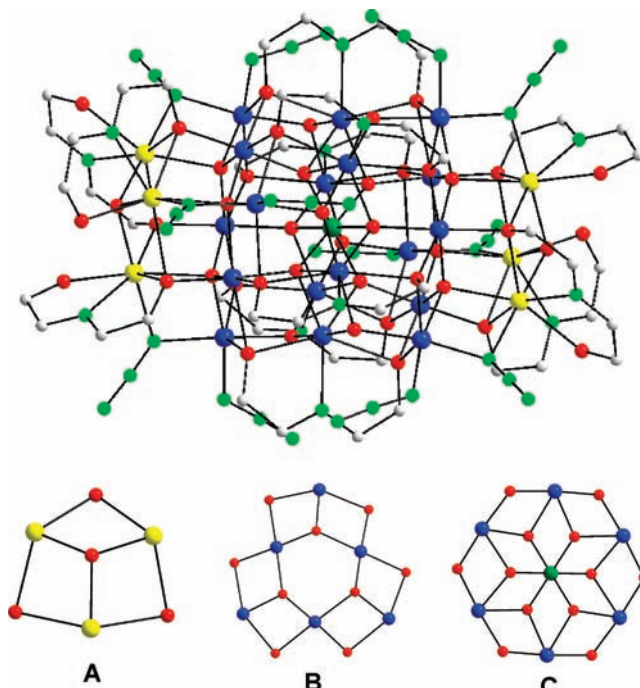

Figure 6. Molecular structure of the cation of **7** (top) and the three types of constituent layers of its core (bottom). Only the *ipso*-C atoms of the pdm^{2-}/pdmH$^-$ phenyl groups are shown. H atoms have been omitted for clarity. Color scheme: Mn^{II}, yellow; Mn^{III}, blue; Mn^{IV}, olive; O, red; N, green; C, gray.

problems from low-lying excited states (Figure 7, top). Despite the small *D*, the compound has a big enough barrier (related to $(S^2 - {}^1/_4)|D|$) to be an SMM, as proven by the appearance of magnetization hysteresis loops below ~ 0.6

Figure 8. Looplike structure of two covalently linked Mn_{12} units in complex **8**. Only the *ipso*-C atoms of the dpkd^{2-} phenyl groups are shown. H atoms have been omitted for clarity. Color scheme: Mn^{II}, yellow; Mn^{III}, blue; O, red; N, green; C, gray.
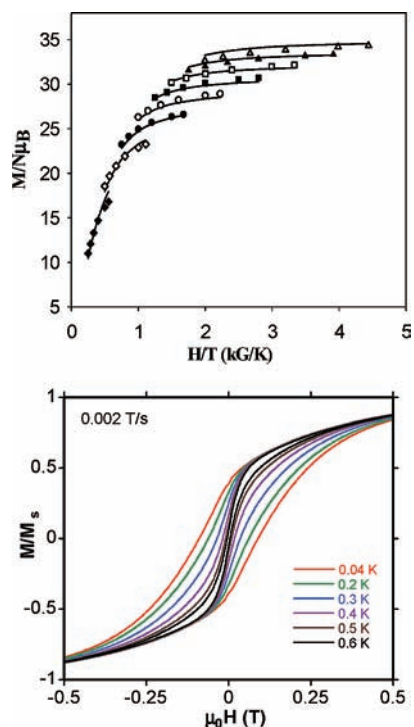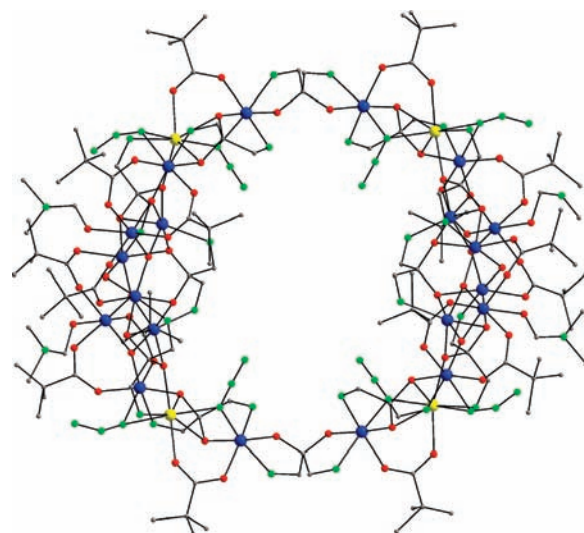
Figure 7. (top) Plot of reduced magnetization ($M/N\mu_B$) vs H/T for complex **7** at applied fields of 0.1–0.8 T and in the 1.8–10 K temperature range. The solid lines are the fit of the data; see the text for the fit parameters. (bottom) Magnetization (M) vs dc field hysteresis loops for complex **7** at the indicated field scan rates and temperatures. The magnetization is normalized to its saturation value, M_s.

K (Figure 7, bottom). Unlike the previous Mn_4 and Mn_{10} complexes, it is not possible to rationalize the large $S = {}^{51}/_2$ ground state on the basis of predicted spin alignments, because there are simply too many triangular subunits within the structure, both within the five layers and between layers, and many of these will involve competing antiferromagnetic $Mn^{II}Mn^{III}$ and $Mn^{III}Mn^{III}$ interactions. The resulting spin alignments will thus be very sensitive to the relative magnitude of these competing interactions. Probably the only safe prediction that can be made is that the central layer of six Mn^{III} atoms surrounding a central Mn^{IV} atom (Figure 6, layer **C**) will have an $S = {}^{21}/_2$ subunit spin, resulting from strong $Mn^{III}Mn^{IV}$ interactions dominating the weaker $Mn^{III}Mn^{III}$ interactions and aligning all of the Mn^{III} spins parallel to each other and antiparallel to the central Mn^{IV} spin, giving $S = 12 - {}^3/_2 = {}^{21}/_2$. This putative large spin of the central layer **C** then represents a foundation for the overall large spin of the molecule, which is determined by the exact nature and relative magnitude of all of the other ferro- and antiferromagnetic interactions in the molecule.[17a] The low anisotropy of the molecule ($D = -0.020$ cm^{-1}) can, however, be rationalized from a consideration of the relative orientations of the 18 Mn^{III} JT elongation axes. These are found to be essentially equally oriented among the *x*, *y*, and *z* directions; i.e., there is no preferential orientation and thus little net molecular anisotropy. Nevertheless, there is enough to make the compound an SMM, given the abnormally large S value.

A.1.3. Di-2-pyridyl Ketone (dpk). As an extension to the work with bidentate (N,O) hmp$^-$ and tridentate (N,O,O) pdmH$^-$/pdm^{2-}, which yielded the Mn_{10} ($S = 22$) and Mn_{25} ($S = {}^{51}/_2$) complexes described above, we have more recently

explored Mn reactions with azide and the potentially tetradentate (N,N,O,O) *gem*-diolate of di-2-pyridyl ketone, $(py)_2C(O)_2^{2-}$ (dpkd^{2-}), formed in situ from dpk [dpk = $(py)_2CO$; dpkdH$_2$ = $(py)_2C(OH)_2$; Scheme 2]. We considered dpkd^{2-} particularly attractive because it can be considered the fusion of two hmp$^-$ groups (Scheme 2). Thus, we have investigated a number of reactions between Mn reagents, NaN$_3$, and dpk under a variety of conditions. The $Mn(ClO_4)_2 \cdot 6H_2O$, NaO_2CBu^t, dpk, NEt$_3$, and NaN$_3$ (1:2:1: 1:1 molar ratio) reaction system in MeCN/DMF gave a dark-brown solution from which was subsequently isolated $[Mn_{24}O_{10}(N_3)_8(O_2CBu^t)_{16}(dpkd)_{12}(DMF)_4]$ (**8**). The analogous reaction with MeCO$_2^-$ in place of Bu^{t}CO$_2^-$ gave instead $[Mn_{26}O_8(OH)_4(N_3)_{12}(O_2CMe)_6(dpkd)_{14}(DMF)_4]$ (**9**).[33] Complex **8** (Figure 8) is a mixed-valent ($Mn^{II}_4Mn^{III}_{20}$) centrosymmetric Mn_{24} loop with a saddle-shaped (closed sinusoidal) conformation and containing eight end-on $\eta^1:\eta^1:\mu$-N$_3^-$ ions; there are two approximately semicircular Mn_{12} units linked covalently but via two long, four-bond connections each involving a $\eta^1:\eta^1:\eta^1:\eta^1:\mu$-dpkd^{2-} group. (In this and examples to follow, where we are describing the binding mode of a polydentate ligand, we shall use the η label to indicate the number of metal atoms to which each donor atom of that ligand is bound rather than employing other available conventions.) Complex **9** is again mixed-valent ($Mn^{II}_{12}Mn^{III}_{14}$) and also comprises two identical, covalently linked units; in this case, two Mn_{13} units are connected by two end-on $\eta^1:\eta^1:\mu$-N$_3^-$ ions to give a dumbbell structure (Figure 9). Each Mn_{13} unit consists of a $Mn^{II}_4Mn^{III}_4$ rodlike subunit attached on either side to $[Mn^{III}_2(\mu$-OR)$_2]$ and $[Mn^{II}Mn^{III}(\mu$-OR)$_2]$ dinuclear units. The latter are additionally bridged to another, central Mn^{II} atom, and these are end-on bridged by the central N$_3^-$ groups connecting the halves of the molecule. The complex contains four types of dpkd^{2-} groups: $\eta^1:\eta^2:\eta^3:\eta^1:\mu_5$, $\eta^1:\eta^1:\eta^3:\eta^1:\mu_4$, $\eta^1:\eta^2:\eta^1:\eta^1:\mu_3$, and η^1:

(33) Stamatatos, Th. C.; Abboud, K. A.; Wernsdorfer, W.; Christou, G. *Angew. Chem., Int. Ed.* **2008**, in press and references cited therein.
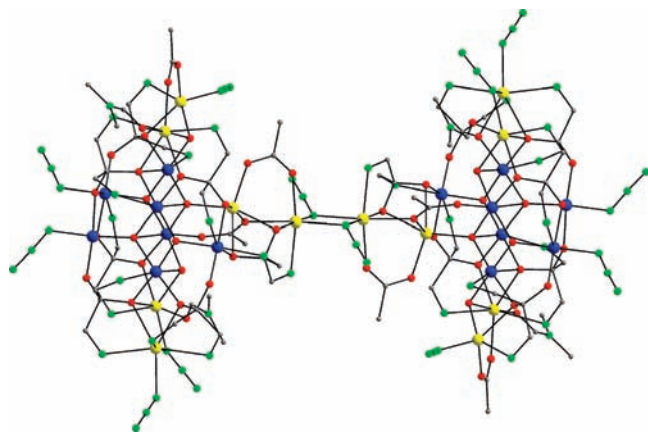
Figure 9. Dumbbell-shaped structure of complex **9**. Color scheme: Mn[II], yellow; Mn[III], blue; O, red; N, green; C, gray. Only the *ipso*-C atoms of the phenyl groups of dpkd[2−] ligands are shown. H atoms have been omitted for clarity.
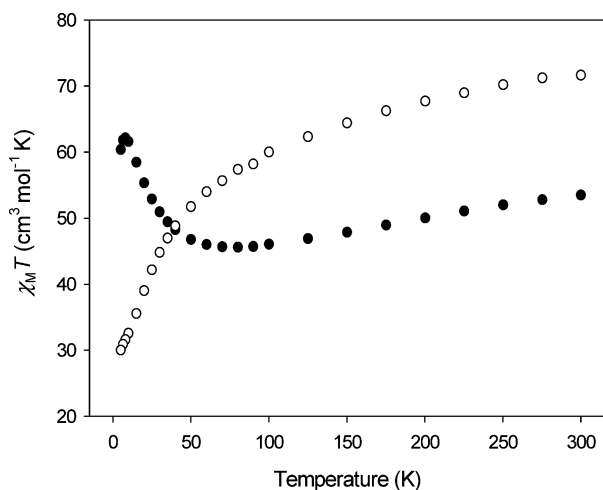

Figure 10. $\chi_M T$ vs T plots for complexes **8** (●) and **9** (○) in a 1 kG field.

Figure 11. Plot of the in-phase (χ'_M) (as $\chi'_M T$) and out-of-phase (χ''_M) ac susceptibility signals of complex **9**, measured in a 3.5 G field oscillating at the indicated frequencies.

$\eta^2:\eta^2:\eta^1:\mu_4$, emphasizing the bridging flexibility of this group.

The solid-state dc magnetic susceptibility data (χ_M) for **8** and **9**, plotted as $\chi_M T$ vs T in Figure 10, reveal both complexes to possess relatively large ground-state S values, as targeted by the choice of ligands. Attempts to determine the ground states of the complexes by fitting magnetization (M) data collected at various fields and at low temperature (<10 K) were hindered by low-lying excited states, a very common problem in such high-nuclearity complexes. However, ac susceptibility data collected in the 1.8−15 K range with a 3.5 G ac field oscillating at 5−1500 Hz avoided these complications and allowed the ground states of **8** and **9** to be identified as $S = 7$ and 8, respectively. The representative ac plot for **9** is shown in Figure 11: $\chi_M'T$ only slightly decreases with a decrease in the temperature in the 4−15 K region, indicating little population of excited states in this temperature range. At lower temperatures, the plot for **9** (and **8**) displays a frequency-dependent decrease in $\chi_M'T$ and a concomitant appearance of out-of-phase χ_M'' signals, indicating the slow magnetization relaxation of a superparamagnet-like particle; those for **8** are centered below the operating limit of our magnetometer (1.8 K), but those for **9** are entirely visible (Figure 11, bottom), a very rare situation for a high-
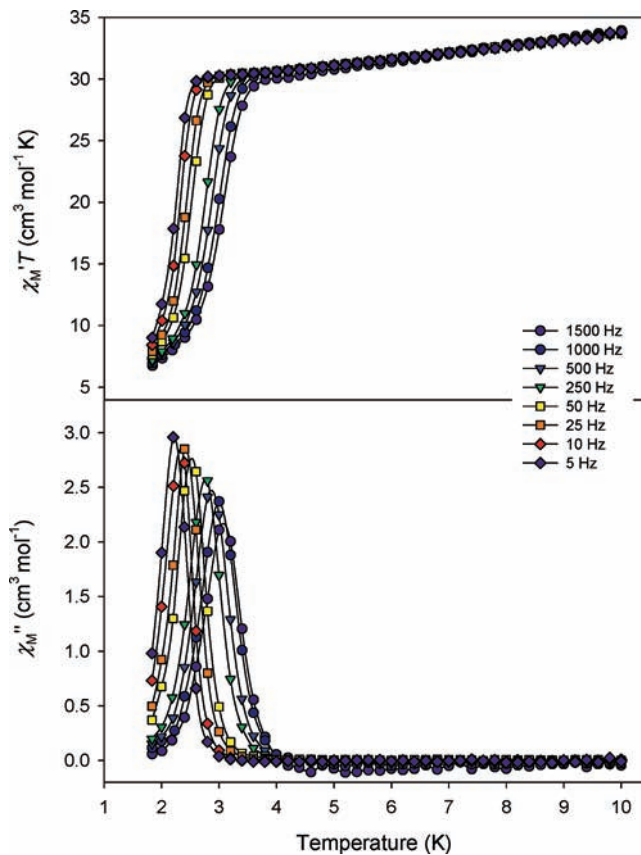
nuclearity Mn[II]/Mn[III] cluster[34] and indicative of a significant barrier (U_{eff}) to magnetization relaxation. An Arrhenius plot constructed from the ac χ_M'' vs T data gave $U_{eff} = 46$ K and $\tau_0 = 3.4 \times 10^{-11}$ s, where τ_0 is the preexponential factor (Figure 12, top); U_{eff} of 46 K is the highest yet observed for a Mn[II]/Mn[III] mixed-valent complex. The ac data thus suggested **8** and **9** to be new SMMs, and this was confirmed for both complexes by magnetization versus dc field scans on single crystals using an array of micro-SQUIDs. These scans exhibited magnetization hysteresis loops, the diagnostic property of a magnet, below 0.8 K for **8** and 1.0 K for **9** (Figure 12, bottom). The loops do not show the steps characteristic of QTM, except for the one at zero field in Figure 12. This is the usual case for large SMMs because they are more susceptible to step-broadening effects from low-lying excited states, intermolecular interactions, and distributions of local environments owing to ligand and solvent disorder. No sign of an exchange bias was observed in the loops, indicating that **8** and **9** behave magnetically as single SMMs rather than as weakly coupled [Mn_12]_2 and [Mn_13]_2 dimers, respectively; a true exchange bias has been previously observed in the hydrogen-bonded [Mn_4]_2 and [Fe_9]_2 dimers.[35]

(34) For the only previously reported high-nuclearity Mn[II]/Mn[III] cluster with clear out-of-phase (χ_M'') peaks and a large U_{eff} barrier, see: (a) Maheswaran, S.; Chastanet, G.; Teat, S. J.; Mallah, T.; Sessoli, R.; Wernsdorfer, W.; Winpenny, R. E. P. *Angew. Chem., Int. Ed.* **2005**, *44*, 5044.
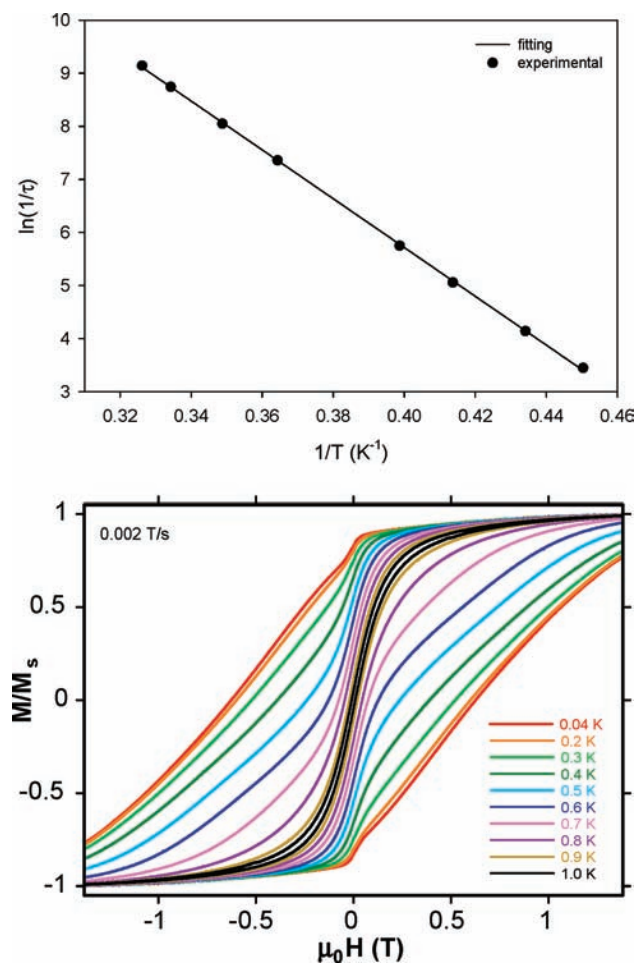
Figure 13. Molecular structure of complex **10**, with H atoms omitted for clarity. Color scheme: Mn^{II}, yellow; Mn^{III}, blue; O, red; N, green; C, gray.

Figure 12. (top) Plot of relaxation time (τ) vs $1/T$ using ac χ''_M data for complex **9**. The solid line is the fit of the data to the Arrhenius equation. See the text for the fit parameters. (bottom) Magnetization (M) vs applied dc field (H) hysteresis loops for single crystals of **9·**solv at the indicated temperatures. The magnetization is normalized to its saturation value (M_s).

Figure 14. Plot of $\chi_M T$ vs T for complex **10** in a 1 kG dc field.

Replacement of MeCN by MeOH in the reaction mixture that gave **9** led instead to the one-dimensional chain composed of $[Mn^{II}_4Mn^{III}_2(N_3)_4(O_2CMe)_2(dpkd)_2(dpk\text{-}met)_2(MeOH)_2]$ (**10**) repeating units,[36] where dpk-met^{2-} is the dianion of a new form of dpkd^{2-}. The structure of the Mn_6 unit (Figure 13) comprises a central, planar $[Mn^{II}_2Mn^{III}_2]$ rhombus bridged by two $\eta^1{:}\eta^1{:}\mu\text{-}N_3^-$ ions and the alkoxide arms (RO$^-$) of two each of dkpd^{2-} and dpk-met^{2-} ligands. The rhombus is additionally linked to two extrinsic Mn^{II} atoms by two RO$^-$ and MeCO$_2^-$ groups. Each Mn_6 unit is bridged to the adjacent ones through two $\eta^1{:}\eta^1$ (end-on) N_3^- ions to give an overall one-dimensional chain. dc magnetic susceptibility studies of **10** (Figure 14) reveal predominantly antiferromagnetic intra-Mn_6 interactions, and strong ferromagnetic inter-Mn_6 interactions as expected through the azide groups. Combined ac data and single-crystal magnetic studies at low temperatures have confirmed **10** to be a new addition in the family of single-chain magnets (SCMs), with a
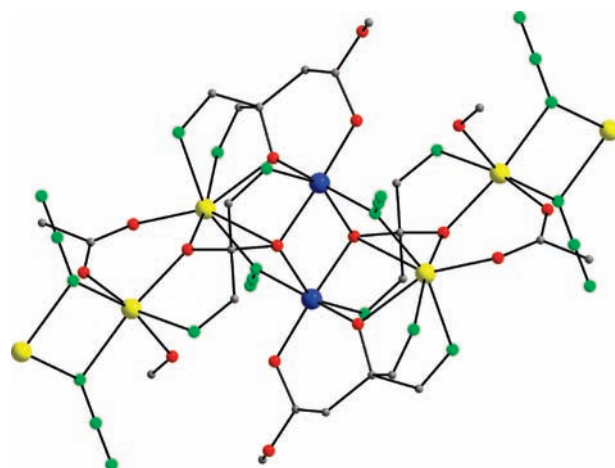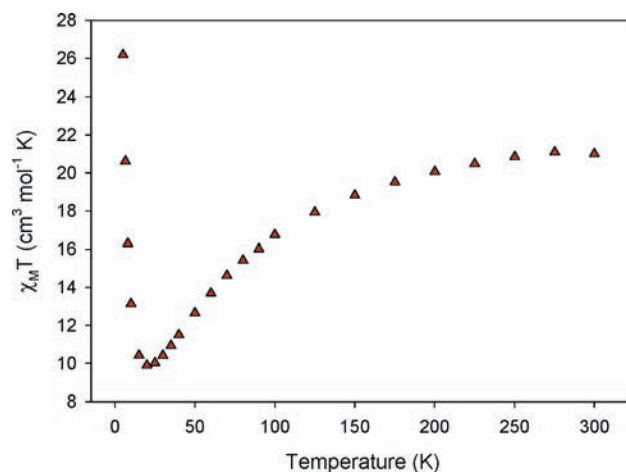
relatively large Δ value (related to $(8J + |D|)S^2$) and a strongly ferromagnetic inter-Mn_6 interaction ($J > 0$).

It should be noted that use of azide ions for the preparation of SCMs is with precedent, having been reported in Co^{II} [37] and Mn^{III} [38] chemistry by Gao and co-workers and in mixed-valent Mn^{II}/Mn^{III} chemistry by Miyasaka, Clérac and co-workers.[23d] In all of these, the N_3^- ions act exclusively as the linker groups between the repeating mononuclear[37] or Mn_x ($x = 3$ or 4)[23d,38] magnetic units to give chains. Thus, complex **10** differs from these previous examples of azide-containing SCMs in both its larger Mn_x nuclearity and in the fact that its azide groups do not just link different Mn_6 clusters into chains but also occur within the repeating clusters.

A.2. Non-Pyridyl Alcohols. A.2.1. *N*-**Methyldiethanolamine (mdaH$_2$).** There are currently no examples of end-on bridging N_3^- ions in Mn/mdaH$_2$ cluster chemistry, and this area merits further investigation. Our own work with this combination has, however, resulted in an example containing terminally bound azide ions. The reaction of a

(35) (a) Wernsdorfer, W.; Aliaga-Alcalde, N.; Hendrickson, D. N.; Christou, G. *Nature* **2002**, *416*, 406. (b) Bagai, R.; Wernsdorfer, W.; Abboud, K. A.; Christou, G. *J. Am. Chem. Soc.* **2007**, *129*, 12918.

(36) Stamatatos, Th. C.; Abboud, K. A.; Wernsdorfer, W.; Christou, G. Manuscript in preparation.

(37) Liu, T.-F.; Fu, D.; Gao, S.; Zhang, Y.-Z.; Sun, H.-L.; Su, G.; Liu, Y.-J. *J. Am. Chem. Soc.* **2003**, *125*, 13976.

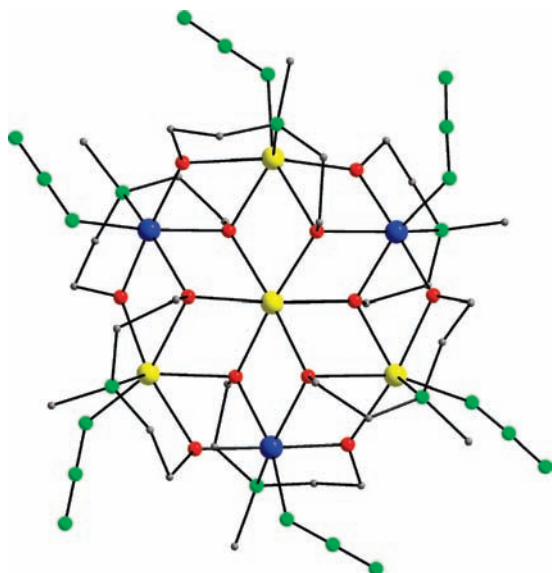(38) Xu, H.-B.; Wang, B.-W.; Pan, F.; Wang, Z.-M.; Gao, S. *Angew. Chem., Int. Ed.* **2007**, *46*, 7388.

Figure 15. Molecular structure of the anion of complex **11**, with H atoms omitted for clarity. Color scheme: Mn^{II}, yellow; Mn^{III}, blue; O, red; N, green; C, gray.
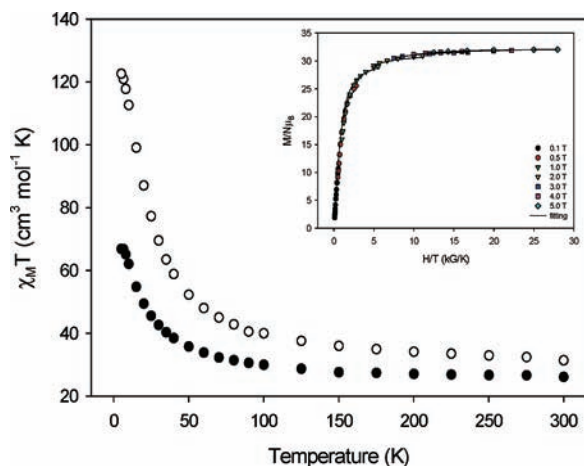

Figure 16. $\chi_M T$ vs T plots for complexes **11** (●) and **12** (○) in a 1 kG field. Inset: Plot of $M/N\mu_B$ vs H/T for **12** at the indicated fields. The solid lines are the fit of the data; see the text for the fit parameters.

Mn^{2+} salt, mdaH$_2$, NEt$_3$, and NaN$_3$ in DMF/MeOH gave $\{[Na(MeOH)_3][Mn_7(N_3)_6(mda)_6]\}_n$ (**11**) repeating units.[39] The structure of the $[Mn_7(N_3)_6(mda)_6]^-$ anion (Figure 15) consists of six Mn atoms (3 Mn^{II} and 3 Mn^{III}) arranged in a nearly planar ring around a central, seventh Mn^{II} atom. The Mn atoms are held together by the 12 O atoms of 6 η^2:η^1: η^3:μ_4-mda^{2-} groups, with the η^3-O atoms linking the Mn$_6$ hexagon and the central Mn atom. Peripheral ligation about the Mn$_7$ anion is provided by the six terminal N$_3^-$ ions.

Solid-state dc magnetic susceptibility studies reveal that the anion of complex **11** possesses an intermediate $S = 11$ spin ground state (Figure 16), which was confirmed by the fitting of magnetization (M) data collected in the 0.1−5 T and 1.8−10.0 K ranges by matrixdiagonalization, and including axial zero-field splitting ($D\hat{S}_z^2$), the Zeeman interaction, and a full powder average. The fitting gave $S = 11$, $g = 1.95$, and $D = -0.15$ cm^{-1}. The $S = 11$ ground

(39) Stamatatos, Th. C.; Poole, K. M.; Foguet-Albiol, D.; Abboud, K. A.; O'Brien, T. A.; Christou, G. *Inorg. Chem.* **2008**, *47*, 6593.
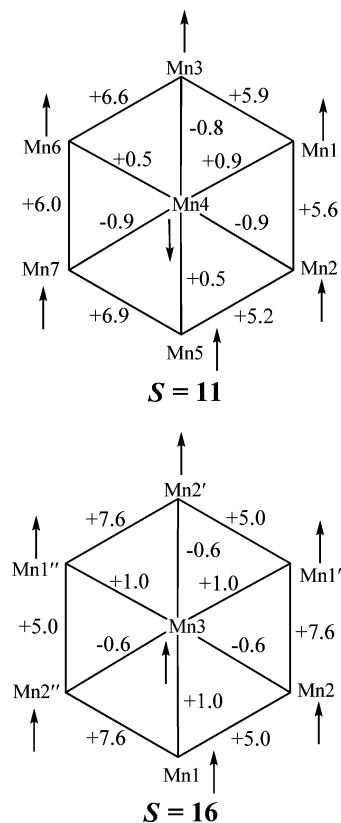
**Figure 17.** Calculated J values obtained by DFT of the anions of **11** (top) and **12** (bottom) using the $H = -2J_{ij}\hat{S}_i\cdot\hat{S}_j$ convention, and the resulting ground-state spin alignments. The atom labels are those related to the crystallographic CIF files.

state of this complex, which is the same as that seen for other nonazide Mn$_7$ complexes with the same structure and oxidation states,[23a,f,27b] was rationalized by theoretical (DFT) calculations using the crystallographic coordinates. The calculated pairwise Mn$_2$ exchange parameters J_{ij} are summarized pictorially in Figure 17 (top) and clearly explain the $S = 11$ state on the basis of spin frustration. The outer J(Mn^{2+},Mn^{3+}) interactions are all ferromagnetic and significantly stronger than the inner J(Mn^{2+},Mn^{2+}) and J(Mn^{2+},Mn^{3+}) interactions, aligning all outer spins parallel. The alignment of the central Mn^{2+} spin is thus determined by the relative magnitude of $J_{22(i)}$ and $J_{23(i)}$ of different sign (i = inner; o = outer); the former is the stronger, frustrating the latter and aligning the spin antiparallel to the outer hexagon; this spin-up/spin-down arrangement clearly explains the observed $S = 11$ ground state for **11** and related compounds. The spin alignments of Figure 17 (top) are confirmed by the calculated spin couplings $\langle \hat{S}_i \cdot \hat{S}_j \rangle$.[39]

A.2.2. Triethanolamine (teaH$_3$). The ternary Mn/N$_3^-$/teaH$_3$ reaction system in a DMF/MeOH solvent mixture has led to a product structurally similar to complex **11** but with extremely interesting differences in magnetic properties. The complex is $\{Na[Mn_7(N_3)_6(teaH)_6]\}_n$ (**12**; Figure 18), and its Mn$_7$ anion is essentially isostructural with that of **11** except for the mda^{2-} vs teaH^{2-} difference, with the third alcohol arm of the latter group being protonated and bound to the Na$^+$ ion rather than Mn; the six N$_3^-$ ions are again terminally
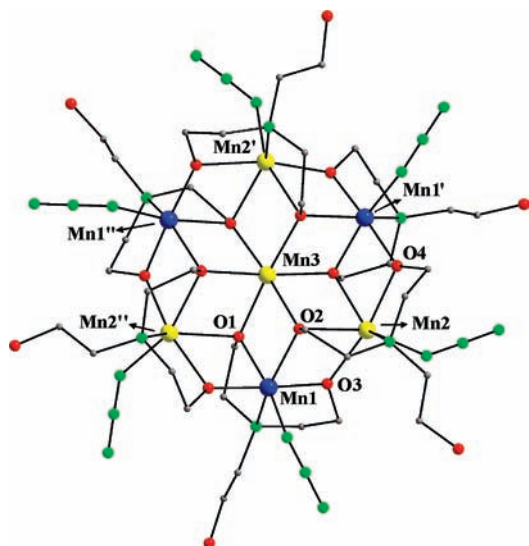
Figure 18. Molecular structure of the anion of complex **12**, with H atoms omitted for clarity. Color scheme: Mn^{II}, yellow; Mn^{III}, blue; O, red; N, green; C, gray.

bound. The magnetic properties of the anion of **12** are, however, distinctly different from those of **11**: $\chi_M T$ rapidly increases to a maximum value of 122.63 cm^3 K mol^{-1} at 5.0 K (Figure 16), indicating a much larger ground state S than that for **11**. Fitting of magnetization data gave $S = 16$, $g = 1.95$, and $D = -0.02$ cm^{-1} (Figure 16, inset). The $S = 11$ vs $S = 16$ difference for **11** vs **12** was further supported experimentally by in-phase ac susceptibility data in the 1.8−15 K range using a 3.5 G ac field oscillating at 5−1500 Hz. The origin of the $S = 16$ ground state was rationalized by a DFT calculation, and the results are summarized in Figure 17 (bottom). The main and crucial difference is that the relative magnitudes of $J_{22(i)}$ and $J_{23(i)}$ have reversed, with the ferromagnetic $J_{23(i)}$ now being stronger, aligning the central spin parallel to the outer hexagon; this spin-up/spin-up situation between the outer hexagon and inner Mn atom gives the maximum possible $S = 16$ ground state for **12**. Small structural changes from the different ligand sets, different packing arrangements, forces, etc., have clearly caused the switch in the ground state by small changes to $J_{22(i)}$ and $J_{23(i)}$.[39]

More recently, an even higher nuclearity, mixed-valence Mn^{II}/Mn^{III} cluster has been obtained from the further study of the $Mn/N_3^-/teaH_3$ reaction system, namely, $[Mn^{II}_3Mn^{III}_{15}$-$O_{11}(OH)(OMe)(N_3)_{12}(tea)_3(teaH)_3(MeOH)]$ (**13**).[40] The core of complex **13** can be dissected into three layers, **ABC**, of different sizes (Figure 19). All three layers can be described as comprising fused $[Mn_3O]$ triangular units: layer **A** is a Mn^{III}_4 rhombus, layer **B** is a large Mn^{III}_6 triangle comprising three corner-sharing Mn^{III}_3 triangles, and layer **C** consists of a $Mn^{III}_5Mn^{II}_2$ disklike unit (somewhat similar to those in **11** and **12**) connected to an additional, extrinsic Mn^{II} atom. Each layer is held together and linked to its neighboring layers by a combination of oxide, alkoxide, and azide ligands. The azide ions are arranged into three classes, emphasizing
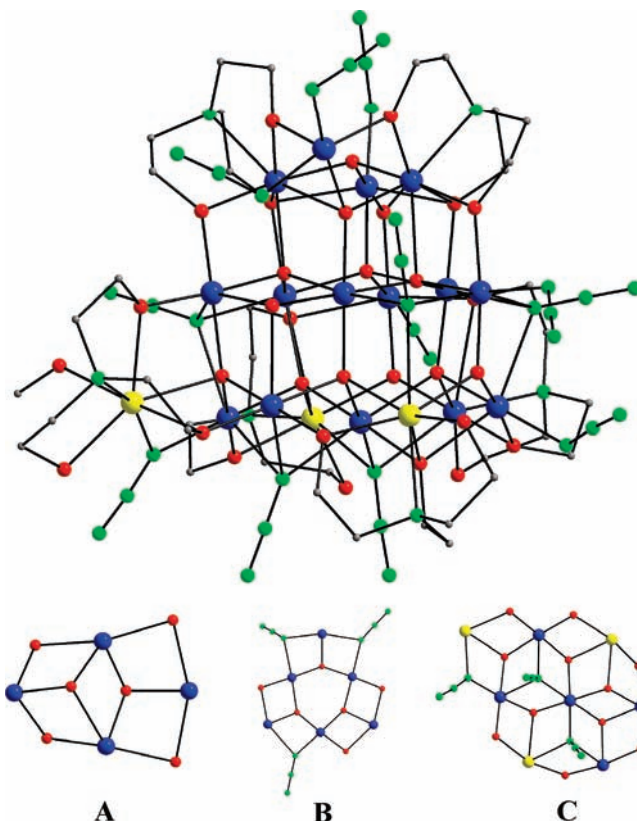
(40) Stamatatos, Th. C.; Foguet-Albiol, D.; Abboud, K. A.; Wernsdorfer, W.; Christou, G. To be submitted.

Figure 19. Molecular structure of complex **13** (top) and the three types of layers of its core (bottom). Color scheme: Mn^{II}, yellow; Mn^{III}, blue; O, red; N, green; C, gray. H atoms have been omitted for clarity.

their coordinating versatility and flexibility in Mn cluster chemistry: (i) five of them bind in a μ_3-1,1,1 (end-on) fashion, two bridging a Mn^{II}···Mn^{III} pair and three a Mn^{III}···Mn^{III} pair; (ii) one binds in a μ-1,1 (end-on) fashion, bridging a Mn^{II}···Mn^{III} pair; (iii) the remaining six are each terminally bound to a Mn atom. Complex **13** has a relatively large ground-state spin value $S = {}^{21}/_2$ and is a SMM, one with a new structural motif in Mn-based SMM chemistry.

A.2.3. 1,1,1-Tris(hydroxymethyl)ethane (thmeH₃). Studies by Brechin and co-workers of the $Mn/N_3^-/thmeH_3$ reaction system have led to the structurally very interesting complex $[Mn^{II}_{24}Mn^{IV}_8(thme)_{16}(bpy)_{24}(N_3)_{12}(O_2CMe)_{12}]^{8+}$,[41] whose cation consists of eight $\{Mn_4\}$ metal-centered triangles (also called "metal stars") linked together to form a truncated cube. Eight of the N_3^- ions bind in a μ-1,1 (end-on) fashion, bridging a Mn^{II}···Mn^{II} pair, while the remaining four are terminally bound to four peripheral Mn^{II} atoms. When the closely related ligand 1,1,1-tris(hydroxymethyl)propane (tmpH₃) was employed in place of thmeH₃, the product was now the cluster $[Mn^{II}_{18}Mn^{IV}_6(tmp)_{12}(bpy)_{24}(N_3)_6$-$(O_2CMe)_6]^{12+}$.[42] In this case, the cation consists of only six $\{Mn_4\}$ metal-centered triangles linked together to form a hexagonal loop. All six N_3^- ions bind in a μ-1,1 (end-on) fashion, bridging a Mn^{II}···Mn^{II} pair. Initial magnetic studies

(41) Scott, R. T. W.; Parsons, S.; Murugesu, M.; Wernsdorfer, W.; Christou, G.; Brechin, E. K. *Angew. Chem., Int. Ed.* **2005**, *44*, 6540.
(42) Scott, R. T. W.; Milios, C. J.; Vinslava, A.; Lifford, D.; Parsons, S.; Wernsdorfer, W.; Christou, G.; Brechin, E. K. *Dalton Trans.* **2006**, 3161.
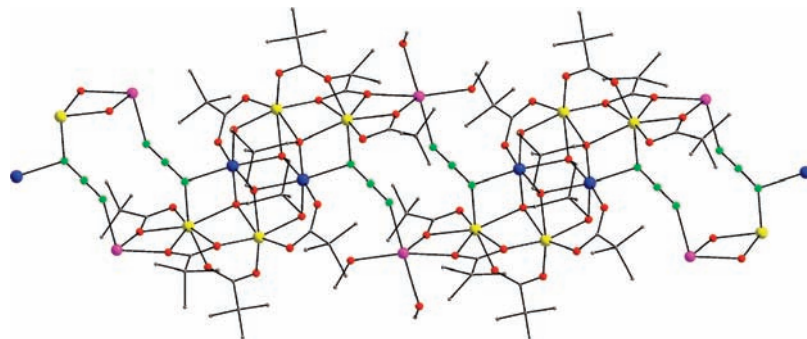
Figure 20. Molecular structure of complex **14**, with H atoms omitted for clarity. Color scheme: Mn^{II}, yellow; Mn^{III}, blue; Na^{I}, purple; O, red; N, green; C, gray.

revealed that both Mn_{32} and Mn_{24} complexes have a spin ground state of $S \approx 9$; unfortunately, the absence of anisotropic Mn^{III} atoms within the complexes precluded the possibility of SMM behavior.

Our own studies of the $Mn/N_3^-/thmeH_3/bpy$ reaction system were carried out without the additional presence of the N,N-chelate bpy, and from one of these reaction systems consisting of a Mn^{II} salt, $thmeH_3$, NaN_3, and NaO_2CBu^t, we were able to isolate the new compound $[Mn^{II}_4Mn^{III}_2Na_2-(O_2CBu^t)_8(N_3)_2(thme)_2(MeOH)_4]$ (**14**).[36] The core of **14** (Figure 20) consists of a central planar Mn_4 rhombus, which is linked to two extrinsic Mn^{II} atoms through the O atoms of two $Bu^tCO_2^-$ groups and a $thme^{3-}$ ligand, and the "head" N atom of two N_3^- ions; the latter bind in a μ-1,1 (end-on) fashion, bridging a $Mn^{II}\cdots Mn^{III}$ pair, while the "tail" N atom of the same group binds to a Na^+ ion, resulting in the formation of one-dimensional $\{[Mn_6]-Na_2-[Mn_6]\}_n$ chains. Thus, the two azido ligands in **14** exhibit a new ligation mode in Mn/Na structural chemistry, i.e., μ-1,1,3 (end-on/end-to-end). The magnetic properties of **14** are currently under investigation and will be reported in due course.

When $EtCO_2^-$ groups were used instead of $Bu^tCO_2^-$, the new complex $[Mn^{II}_2Mn^{III}_4Na_4O(O_2CEt)_5(N_3)(thme)_4]$ (**15**) was obtained in excellent yield.[36] The structure of **15** (Figure 21) consists of a central $[Mn_6(\mu_6-O^{2-})]$ octahedron, linked to four extrinsic Na^+ ions via the O atoms of the $EtCO_2^-$ and $thme^{3-}$ groups. There is only one N_3^- ion present in the molecule, terminally bound to a Mn^{III} atom, so that **15** barely qualifies to be included in this overview, but it is, nevertheless, essential to the formation of complex **15**; in the absence of N_3^-, the corresponding complex with a solvent or another simple ligand at the azide position is not obtained. Preliminary magnetic studies on complex **15** indicate a small but nonzero, ground-state S value but a significant zero-field splitting parameter, D. Additional studies of the $Mn/RCO_2^-/N_3^-/thmeH_3$ reaction system are in progress, and they are revealing this area to be a rich source of new species currently under characterization.

A.2.4. Other Alcohol-Based Ligands. A very interesting result in Mn/azide cluster chemistry was recently reported by Powell and co-workers from the reaction of $MnCl_2$ and 2,6-dihydroxymethyl-4-methylphenol (LH_3) in the presence of NaN_3 and NaO_2CMe. The new $[Mn^{II}_7Mn^{III}_{12}O_8-(N_3)_8(LH)_{12}(MeCN)_6]^{2+}$ cluster consists of two similar Mn_9 fragments that are linked through a central, eight-coordinate
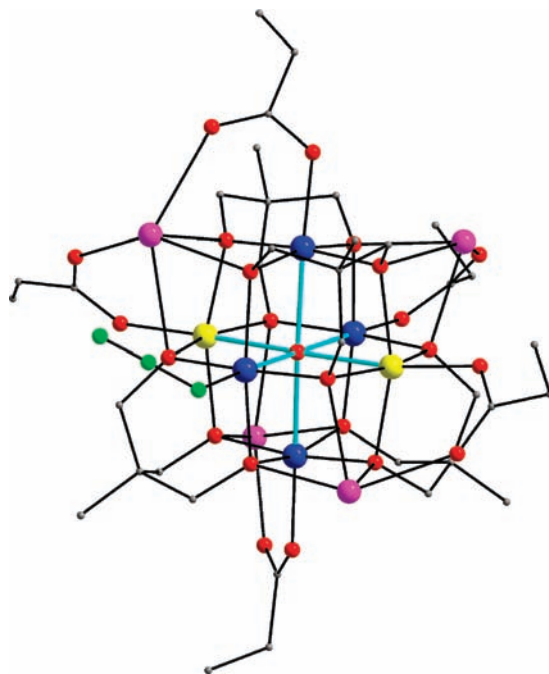

Figure 21. Molecular structure of complex **15**, highlighting with cyan the $[Mn_6(\mu_6-O^{2-})]$ octahedron core. H atoms have been omitted for clarity. Color scheme: Mn^{II}, yellow; Mn^{III}, blue; Na^{I}, purple; O, red; N, green; C, gray.

Mn^{II} atom.[43] The eight $\mu_3-N_3^-$ ions bind in a μ_3-1,1,1 (end-on) fashion, each bridging three Mn^{III} atoms as seen in the Mn_{10} complexes **1** and **2**. The magnetic properties of that complex revealed the complex to possess the maximum possible spin ground state of $S = {}^{83}/_2$ but with essentially no anisotropy, as was expected from the high symmetry and the resulting orientations of the Mn^{III} JT axes; thus, Mn_{19} is not a SMM. Interestingly, more recently a similar Mn_{19} cluster was reported by Kou and co-workers that possesses essentially the same structure but is reported to have a ground-state spin value of $S = {}^{73}/_2$.[44]

The Schiff base family of ligands has long been known to be capable of stabilizing many Mn^{III}-containing compounds, and it thus represents a promising area for new Mn/azide cluster chemistry. Nevertheless, it is one that has been little studied to date for this purpose, and there are conse-

(43) Ako, A. M.; Hewitt, I. J.; Mereacre, V.; Clérac, R.; Wernsdorfer, W.; Anson, C. E.; Powell, A. K. *Angew. Chem., Int. Ed.* **2006**, *45*, 4926.
(44) Ge, C.-H.; Ni, Z.-H.; Liu, C.-M.; Cui, A.-L.; Zhang, D.-Q.; Kou, H.-Z. *Inorg. Chem. Commun.* **2008**, *11*, 675.

quently only a very few reports of polynuclear Mn Schiff base complexes with bridging azido groups. Oshio and co-workers recently published the $\{[Mn^{III}_4(\mu_3\text{-O})(N_3)(sae)_4\text{-}(MeOH)]\text{-}(N_3)\text{-}[Mn^{III}_4(\mu_3\text{-O})(N_3)(sae)_4(MeOH)]\}^+$ cluster (saeH$_2$ is 2-salicylideneaminoethanol), which consists of two identical Mn$^{III}_4$ units connected by a central μ-1,3 (end-to-end) N$_3^-$ ion.[45] The remaining azides, which are within each Mn$_4$ unit, bridge in a μ-1,1 (end-on) fashion. Owing to the end-to-end ligation of the central N$_3^-$ ion, the two Mn$_4$ units are antiferromagnetically coupled with a resulting overall $S = 0$ ground state. Employing slightly different Schiff bases and reaction conditions, Powell and co-workers have reported tetranuclear $[Mn^{II}Mn^{III}_3NaO(N_3)_{2.7}(O_2CMe)_{1.3}L_3(MeOH)]$ and $\{[Mn^{III}_4NaO(N_3)_3L'_4(MeOH)]\}_2^{2+}$ complexes (L and L' are the Schiff base dianions) with distorted trigonal-bipyramidal metal topologies.[46] In both complexes, two bridging N$_3^-$ ions bind in a μ-1,1 (end-on) fashion, each bridging two Mn^{III} atoms, while the remaining azido group is terminally bound to a Mn^{III} atom in the former Mn$^{II/III}_4$ complex, with μ-1,3 (end-to-end) bridging in the latter Mn$^{III}_4$ complex, forming a weak $\{Mn_4\}_2$ dimer. The magnetic studies indicate predominantly antiferromagnetic interactions within the molecules and $S = 1/2$ and 0 ground states, respectively.

B. Manganese Clusters of Azides and Oximato-Based Ligands. B.1. Pyridyl Monoximes. There is currently a renewed interest in the coordination chemistry of oximato-based ligands.[47] The research efforts are driven by a number of considerations, such as their employment in the synthesis of homometallic and heterometallic clusters with interesting magnetic properties, including SMMs and SCMs, and a variety of other potential applications.[48] Ligands containing one oxime, one pyridyl, and no other donor group are popular, and most of these contain a 2-pyridyl group. Once deprotonated, such ligands can bridge two or three metal atoms, exhibiting a strong tendency to stabilize the higher metal oxidation states (i.e., III and IV).[47,48] We have therefore considered it attractive to explore the combination of 2-pyridyl oximes and azides in Mn cluster chemistry, avoiding the copresence of carboxylate groups.

B.1.1. Methyl-2-pyridyl Ketone Oxime (mpkoH). The reaction of a Mn^{II} salt, mpkoH (Scheme 2), and NaN$_3$ gave a dark-red solution from which was obtained the $[Mn^{II}Mn^{III}_5O_3(N_3)_3(mpko)_6(H_2O)_3]^{2+}$ (**16**) cluster.[36] The structure of **16** (Figure 22) consists of three vertex-sharing $[Mn_3(\mu_3\text{-O}^{2-})]$ triangular units additionally bridged by oximate ($-NO^-$) and azide groups. Two of the N$_3^-$ ions bind in a μ-1,1 (end-on) fashion, each bridging two Mn^{III} atoms, while the remaining one is terminally bound to a Mn^{III} center. Combined dc and ac magnetic susceptibility studies confirmed an $S = 5/2$ ground state for **16**, and an appreciable $D = -1.41$ cm^{-1} (Figure 23). As a result of the significant S
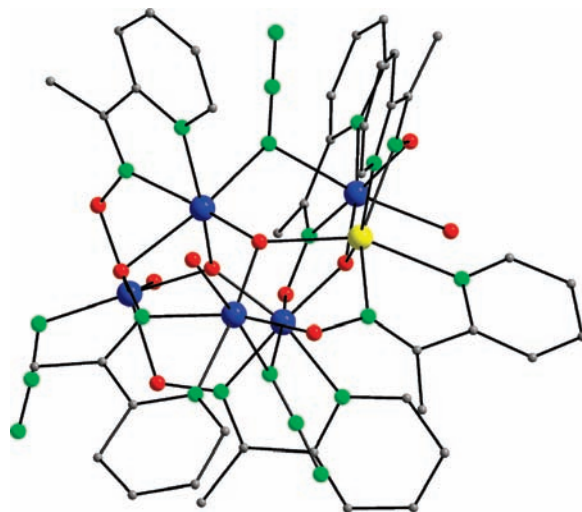
(45) Hoshino, N.; Ito, T.; Nihei, M.; Oshio, H. *Inorg. Chem. Commun.* **2003**, *6*, 377.
(46) Hewitt, I. J.; Tang, J.-K.; Madhu, N. T.; Clerac, R.; Buth, G.; Anson, C. E.; Powell, A. K. *Chem. Commun.* **2006**, 2650.
(47) For a review, see: Chaudhuri, P. *Coord. Chem. Rev.* **2003**, *243*, 143, and references cited therein.
(48) For a review, see: Milios, C. J.; Stamatatos, Th. C.; Perlepes, S. P. *Polyhedron* **2006**, *25*, 134, and references cited therein.

Figure 22. Molecular structure of the cation of complex **16**. H atoms have been omitted for clarity. Color scheme: Mn^{II}, yellow; Mn^{III}, blue; O, red; N, green; C, gray.
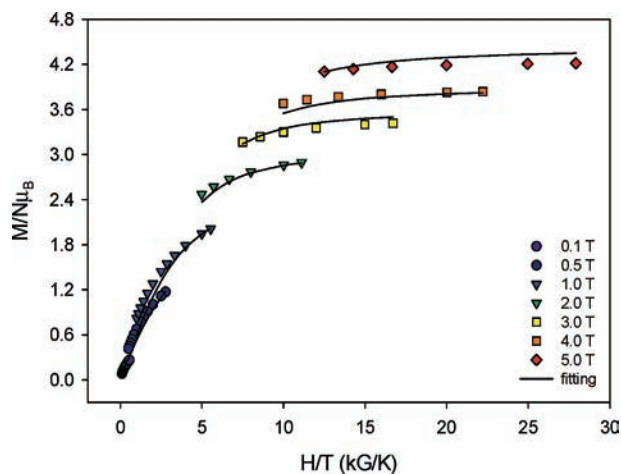

Figure 23. Plot of reduced magnetization ($M/N\mu_B$) vs H/T for complex **16** at applied fields of 0.1−5.0 T and in the 1.8−10 K temperature range. The solid lines are the fits of the data; see the text for the fit parameters.

and D values, the complex exhibits frequency-dependent out-of-phase ac susceptibility (χ_M'') signals, suggesting that **16** is a new half-integer spin SMM. Further studies are in progress.

B.1.2. Phenyl-2-pyridyl Ketone Oxime (ppkoH). Perlepes, Winpenny, and co-workers have employed the bulkier 2-pyridyl oxime ppkoH (Scheme 2) in Mn/azide chemistry, in the presence also of carboxylate ligands, and have obtained the mixed-valent cluster $[Mn^{II}_3Mn^{IV}O(N_3)(O_2CPh)_3\text{-}(ppko)_4]$.[49] It contains an oxide-centered $[Mn_4(\mu_4\text{-O}^{2-})]^{8+}$ tetrahedral core, and the azide group binds in a μ-1,1 (end-on) fashion, bridging two Mn^{II} centers. Fits of magnetic susceptibility data establish the presence of both ferro- and antiferromagnetic interactions and an $S = 6$ ground state.

B.2. Pyridyl Dioximes. B.2.1. 2,6-Diacetylpyridine Dioxime (dapdoH$_2$). As an extension to our work with mpkoH, we have asked what kinds of products might result

(49) Milios, C. J.; Piligkos, S.; Bell, A. R.; Laye, R. H.; Teat, C. J.; Vicente, R.; McInnes, E.; Escuer, A.; Perlepes, S. P.; Winpenny, R. E. P. *Inorg. Chem. Commun.* **2006**, *9*, 638.
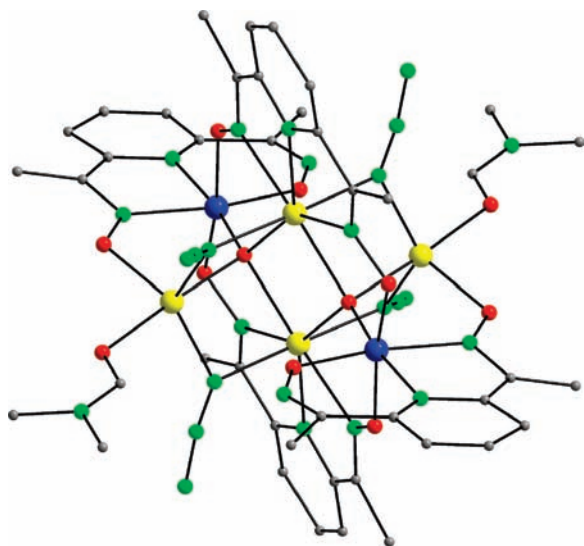
Figure 24. Molecular structure of complex **17**, with H atoms omitted for clarity. Color scheme: Mn^{II}, yellow; Mn^{III}, blue; O, red; N, green; C, gray.
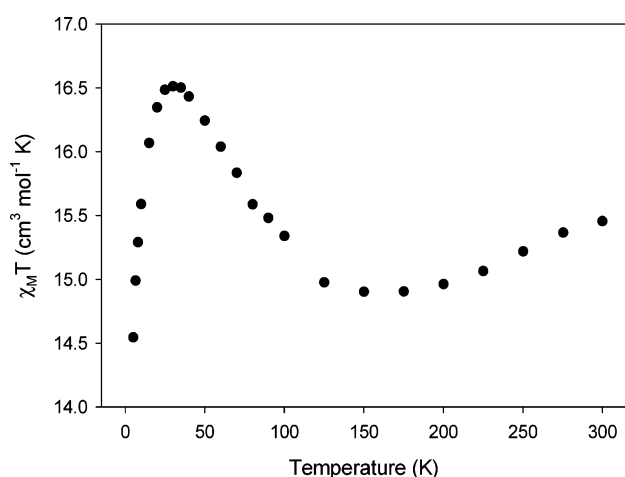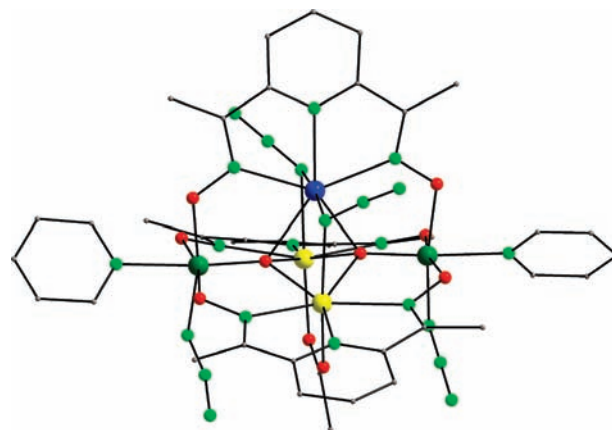

Figure 26. Molecular structure of complex **18**, with H atoms omitted for clarity. Color scheme: Mn^{II}, yellow; Mn^{III}, blue; Mn^{IV}, olive; O, red; N, green; C, gray.
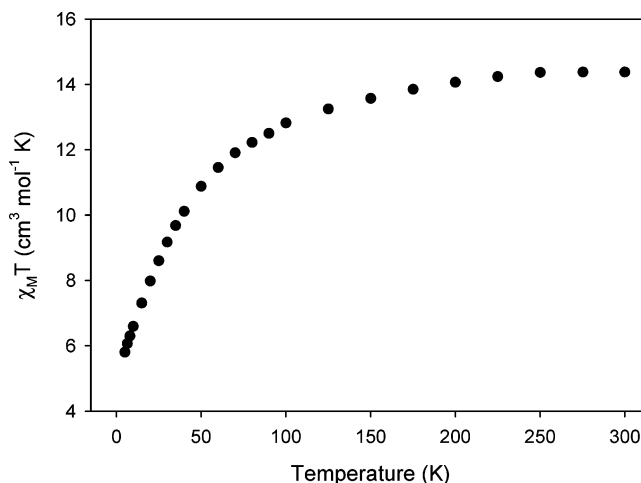

Figure 25. Plot of $\chi_M T$ vs T for complex **17** in a 1 kG dc field.

Figure 27. Plot of $\chi_M T$ vs T for complex **18** in a 1 kG dc field.

from the addition of another ketone oxime arm onto the mpkoH group at the 6 position of the pyridine ring, in the same way that pdmH$_2$ is hmpH with another hydroxymethyl arm at its 6 position. The resulting molecule, 2,6-diacetylpyridine dioxime (dapdoH$_2$), is shown in Scheme 2, where the analogy between the mpkoH/dapdoH$_2$ and hmpH/pdmH$_2$ pairs can be clearly seen. In order to better compare the mpkoH and potential dapdoH$_2$ products, we employed dapdoH$_2$ in the same Mn/azide reaction system that had given complex **16** and obtained [Mn$^{II}_4$Mn$^{III}_2$O$_2$(N$_3$)$_4$(dapdo)$_2$-(dapdoH)$_2$(DMF)$_2$] (**17**). Its structure (Figure 24) consists of an edge-sharing bitetrahedral core, with each tetrahedron containing a central μ_4-O^{2-} ion.[36] All azide groups bind in a μ-1,1 (end-on) fashion, with each bridging two Mn^{II} centers. Combined dc and ac magnetic susceptibility studies have established an $S = 6$ ground state for the complex, which can be rationalized as due to the presence again of both ferro- and antiferromagnetic interactions within **17**, as suggested by the $\chi_M T$ vs T plot profile (Figure 25). Specifically, four ferromagnetically coupled Mn^{II} atoms ($S_{local} = 10$), bridged by four end-on azides and two μ_4-oxides, are antiferromag-

netically coupled to the two extrinsic Mn^{III} atoms; note that the Mn^{II}···Mn^{III} interactions are exclusively promoted by oximato bridges, which usually give antiferromagnetic interactions,[47,48] although occasionally they give ferromagnetic interactions.[12,14]

Using different reaction conditions, the Mn/azide/dapdoH$_2$/carboxylate reaction system yields instead a pentanuclear complex, [Mn$_5$O$_2$(N$_3$)$_4$(O$_2$CMe)(dapdo)$_3$(py)$_2$] (**18**), whose core consists of five Mn ions arranged as a face-sharing bitetrahedron, with each tetrahedron again containing a central μ_4-O^{2-} ion (Figure 26).[36] The complex is a rare mixture of three Mn oxidation states in a low-nuclearity species, containing a Mn$^{II}_2$Mn^{III}Mn$^{IV}_2$ situation, with the Mn^{IV} atoms being the two end ones. Again, two N$_3^-$ ions bind in a μ-1,1 (end-on) fashion, with each bridging a Mn^{II}···Mn^{III} pair, while the remaining two are terminally bound to the two Mn^{IV} centers. Preliminary magnetic studies have revealed predominant antiferromagnetic interactions within **18** (Figure 27) and a resulting $S = 3$ ground state that likely arises from spin-frustration effects and is currently under further study.

Further changes to the reaction solvent and reagent ratio lead to yet a third product in the family, [Mn$^{II}_2$Mn$^{III}_4$-O$_2$(N$_3$)$_8$(dapdo)$_2$(py)$_4$] (**19**). Once again, the structure consists of six Mn ions arranged as an edge-sharing bitetrahedron, with each tetrahedron again containing a central μ_4-O^{2-} ion
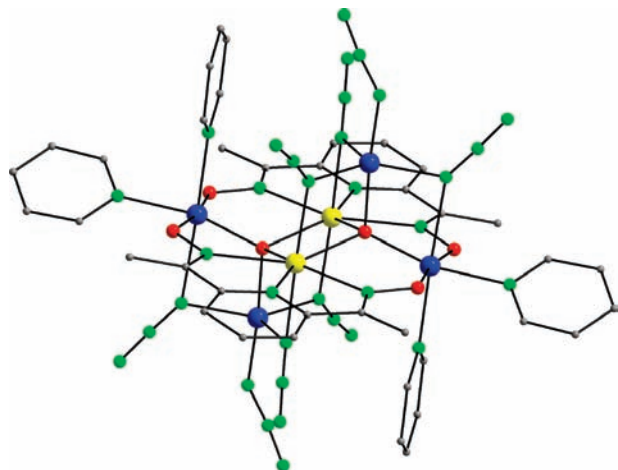
Figure 28. Molecular structure of complex **19**, with H atoms omitted for clarity. Color scheme: Mn^{II}, yellow; Mn^{III}, blue; O, red; N, green; C, gray.

(Figure 28).[36] The eight azides are arranged in two classes: (i) six bind in a μ-1,1 (end-on) fashion, with four bridging Mn^{II}···Mn^{III} pairs and two bridging Mn^{III}···Mn^{III} pairs; (ii) the remaining two are each terminally bound to a Mn^{III} atom. Magnetic studies are currently in progress and will be reported in due course. Note that all three complexes **17**−**19** are mixed-valent species but that they differ significantly in their exact oxidation level: **17** is Mn$^{II}_4$Mn$^{III}_2$, **18** is Mn$^{II}_2$Mn^{III}Mn$^{IV}_2$, and **19** is Mn$^{II}_2$Mn$^{III}_4$, with averages of Mn$^{2.33+}$, Mn^{3+}, and Mn$^{2.67+}$, respectively.

B.3. Non-Pyridyl Oximes. B.3.1. Salicylaldoxime (saoH$_2$) and Its Derivatives (R-saoH$_2$). Tsai and co-workers have recently investigated the Mn/N$_3^-$/saoH$_2$ reaction system and have discovered a [Mn$^{II}_2$Mn$^{III}_3$O(N$_3$)$_6$Cl$_2$(sao)$_3$]$^{3-}$ cluster containing a trigonal-bipyramidal Mn$_5$ core topology.[50] The three Mn^{III} atoms comprise the equatorial triangular plane, which contains a capping μ_3-O^{2-} ion, and the two Mn^{II} atoms occupy the apical positions. Each Mn^{II} atom is linked by three μ-1,1 (end-on) azide bridges to Mn^{III} atoms. The magnetic data of the compound are very interesting, establishing it to contain only ferromagnetic interactions and thus to possess the maximum possible ground state of $S = 11$. In addition, fits of magnetization versus field data reveal a significant anisotropy ($D = -0.22$ cm^{-1}), and this combination of large S and large (and negative) D makes this compound a new SMM, with a significant barrier to magnetization relaxation of $U_{eff} = 40.3$ K.

More recently, Brechin and co-workers have reported octanuclear [Mn$^{II}_2$Mn$^{III}_6$O$_2$(N$_3$)$_6$(R-sao)$_6$(MeOH)$_8$] (R = napth, Me) complexes with similar structures but distinctly different ground-state S values.[51] The core of both molecules consists of a bicapped nonplanar Mn$^{III}_6$ unit of two off-set, stacked [Mn$^{III}_3$(μ_3-O^{2-})]$^{7+}$ triangular subunits. Each of the latter subunits is further capped with one Mn^{II} ion via three μ-1,1 (end-on) N$_3^-$ ions. The magnetic study of the napth analogue

(50) Yang, C.-I.; Wernsdorfer, W.; Lee, G.-H.; Tsai, H.-L. *J. Am. Chem. Soc.* **2007**, *129*, 456.
(51) Milios, C. J.; Inglis, R.; Vinslava, A.; Prescimone, A.; Parsons, S.; Perlepes, S. P.; Christou, G.; Brechin, E. K. *Chem. Commun.* **2007**, 2738.
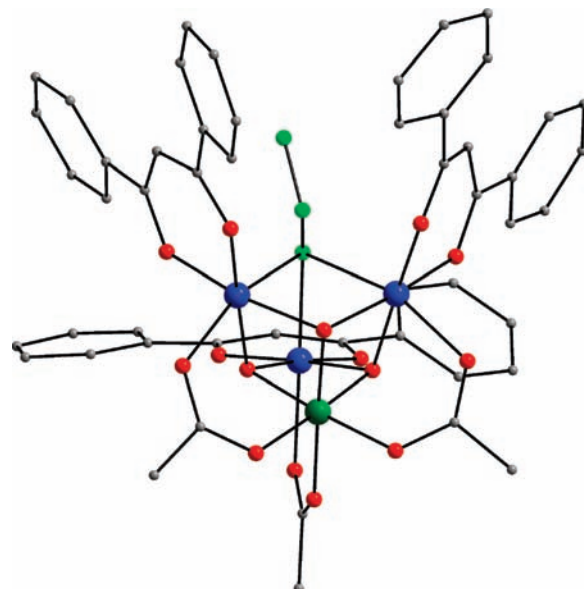
Figure 29. Molecular structure of complex **20**, with H atoms omitted for clarity. Color scheme: Mn^{III}, blue; Mn^{IV}, olive; O, red; N, green; C, gray.

indicated predominantly antiferromagnetic interactions within the molecule and a small ($S \approx 1$) ground state. In contrast, the Me analogue exhibits increased ferromagnetic interactions and a consequently larger $S \approx 7$ ground state, which makes the compound a new SMM.

C. Azides in Manganese Carboxylate Cluster Chemistry. Past and recent attempts to amalgamate azide and carboxylate groups in Mn cluster chemistry without the copresence of an extra bridging/chelate ligand have led to the complexes [Mn$^{III}_3$Mn^{IV}O$_3$(N$_3$)(O$_2$CMe)$_3$(dbm)$_3$] (**20**) (dbm$^-$ is the anion of dibenzoylmethane) and [Mn$^{III}_3$Mn$^{III}_{22}$-O$_{20}$(N$_3$)$_6$(O$_2$CPh)$_{26}$(MeCN)$_2$] (**21**). Complex **20** was, in fact, the first higher oxidation state Mn/azide complex to be prepared and contains a [Mn$^{III}_3$Mn^{IV}(μ_3-O)$_3$(μ_3-N$_3$)]$^{6+}$ very distorted cubane core with a Mn$^{III}_3$Mn^{IV} trigonal-pyramidal topology (Figure 29).[52] The azide group binds in a μ_3-1,1,1 (end-on) fashion, bridging three Mn^{III} atoms. This complex, like the many others with an analogous Mn$^{III}_3$Mn^{IV} distorted-cubane core, possesses an $S = \,^9/_2$ ground state. This is readily explained as a consequence of antiferromagnetic coupling between the Mn^{IV} atom and each of the Mn^{III} atoms and ferromagnetic coupling between the Mn^{III} atoms, as was expected from the end-on ligation of the azido group. As a result, the ground state is $S = 6 - \,^3/_2 = \,^9/_2$. There is thus no spin frustration in this complex. As a consequence, the ground state of **20**, and indeed also those of all of this Mn$_4$ family with the same distorted-cubane [Mn$^{III}_3$Mn^{IV}(μ_3-O^{2-})$_3$(μ_3-X)]$^{6+}$ (X = N$_3^-$, Cl$^-$, Br$^-$, F$^-$, MeCO$_2^-$, etc.), is very isolated from the $S = \,^7/_2$ first excited state, typically by >100 cm^{-1} above the ground state (with the exact energy gap depending on the X group). This is a most unusual situation in Mn/O cluster chemistry. Complex **20** also has a significant anisotropy, as a result of the three Mn^{III} JT elongation axes intersecting at the bridging N$_3^-$ group and

(52) Wemple, M. W.; Adams, D. M.; Hagen, K. S.; Folting, K.; Hendrickson, D. N.; Christou, G. *J. Chem. Soc., Chem. Commun.* **1995**, 1591.
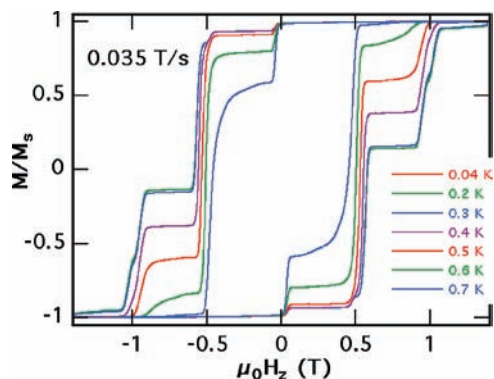
Figure 30. Hysteresis loops for a member of the family of $[Mn_4O_3X(O_2CR)_3(dbm)_3]$ complexes at a field sweep rate of 0.035 T s^{-1} and at the indicated temperatures. The magnetization (M) is normalized to its saturation value, M_S.
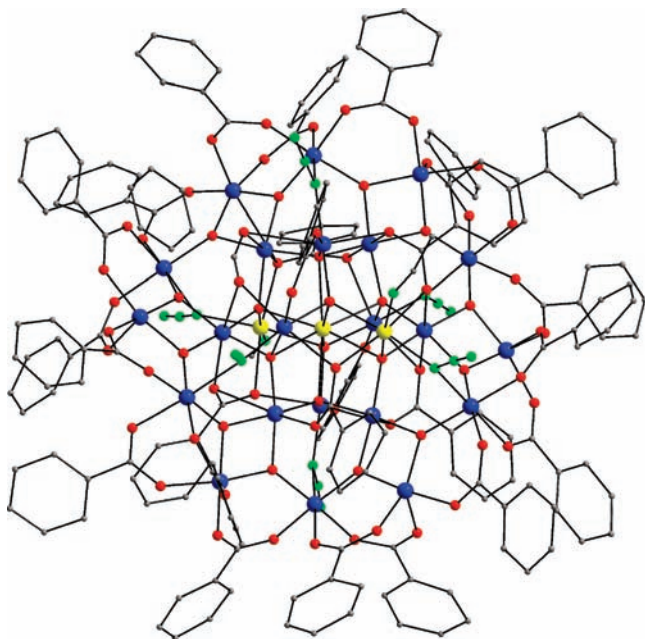

Figure 31. Molecular structure of complex **21**, with H atoms omitted for clarity. Color scheme: Mn^{II}, yellow; Mn^{III}, blue; O, red; N, green; C, gray.

thus projecting a significant overall molecular anisotropy. The combination of significant S and D values results in the Mn$_4$ complexes, and particularly in **20**, being among the smallest SMMs known (Figure 30)[53] and the second most studied group of SMMs after the prototypical $[Mn_{12}O_{12}(O_2CR)_{16}(H_2O)_4]$ family.

Complex **21** (Figure 31) was only very recently obtained and has an unprecedented and remarkable structure. It consists of 25 Mn ions arranged as 6 external, edge-sharing $[Mn^{III}_4(\mu_3-O^{2-})_2]^{8+}$ "butterfly" units linked to 6 internal, edge-sharing $[Mn_4(\mu_4-O^{2-})]$ tetrahedra through oxide and azido ligands.[54] The six N$_3^-$ ions bind in a μ-1,1 (end-on) fashion, two of them bridging a Mn$^{II}\cdots$Mn^{III} and four a Mn$^{III}\cdots$Mn^{III} pair. Peripheral ligation about the Mn/O^{2-} core is provided by 26 η^1:η^1:μ bridging PhCO$_2^-$ groups and two terminal

MeCN molecules. Preliminary magnetic studies indicate predominantly antiferromagnetic interactions within **21**; however, the appearance of out-of-phase (χ''_M) signals suggests that **21** may be a new SMM. Further studies are in progress.

Conclusions

The field of higher oxidation state Mn/azide chemistry began in 1995 with the tetranuclear complex $[Mn^{III}_3Mn^{IV}-O_3(N_3)(O_2CMe)_3(dbm)_3]$ (**20**) with $S = \frac{9}{2}$ but has only recently begun to pick up research momentum. Nevertheless, it has now grown to encompass a variety of metal nuclearities and spin states. Both the structural chemistry and the resulting magnetic properties have proven to be of great interest and would justify their study even in the absence of the other; that both aspects are to be found in combination in this area is thus the best of both worlds. The structural chemistry is replete with molecules of aesthetically pleasing architecture, from beautiful simplicity to fascinating complexity, and everything in-between. Such a situation is one of the benefits that make synthetic chemistry, in general, such an enjoyable and satisfying occupation. The magnetic properties are among the most interesting discovered to date, from new SMMs to extremely high S values and combinations thereof. Indeed, one of the most satisfying aspects of this chemistry with respect to the magnetic properties has been the commonly observed μ-1,1 or μ_3-1,1,1 (end-on) bridging mode of the azide group because this is the one that favors ferromagnetic exchange interactions and thus can facilitate products with a high ground-state S value. This has undoubtedly been one of the main reasons that this area of Mn/azide chemistry is proving such a rich source of molecules with high S values.

We have no reason to believe that this area is exhausted of interesting new results. Indeed, on the basis of our ongoing studies and the results arising from them yet to be published, our own opinion is that we have seen only the tip of the iceberg in this area and that many exciting molecules and properties await discovery.

(53) Aliaga-Alcalde, N.; Edwards, R. S.; Hill, S. O.; Wernsdorfer, W.; Folting, K.; Christou, G. *J. Am. Chem. Soc.* **2004**, *126*, 12503, and references cited therein.
(54) Vinslava, A.; Christou, G. Manuscript in preparation.

IC801217J